

DETERMINATION OF D-MESON LIFETIMES

LEBC-EHS Collaboration

Aachen¹, Bombay², Brussels³, CERN⁴, College de France⁵, Genova⁶,
Japan Universities⁷ (Chuo University, Tokyo Metropolitan University,
Tokyo University of Agriculture and Technology), Liverpool⁸, Madrid⁹, Mons¹⁰,
Oxford¹¹, Padova¹², Paris¹³, Rome¹⁴, Rutherford¹⁵, Rutgers¹⁶, Serpukhov¹⁷,
Stockholm¹⁸, Strasbourg¹⁹, Tennessee²⁰, Torino²¹, Trieste²² and Vienna²³

M. Aguilar-Benitez⁹, W.W. Allison¹¹, J.L. Bailly¹⁰, J.F. Baland¹⁰,
S. Banerjee², W. Bartl²³, M. Begalli¹, P. Belliere⁵, R. Bizzarri¹⁴,
G. Borreani²¹, H. Briand¹³, W.M. Bugg²⁰, V. Canale¹⁴, C. Caso⁶,
E. Castelli²², P. Checchia¹², P. Chliapnikov¹⁷, N. Colino⁹, R. Contri⁶,
D. Crennell¹⁵, L. de Billy¹³, C. Defoix⁵, A. De Angelis¹², R. Dimarco¹⁶,
E. di Capua¹⁴, J. Dolbeau⁵, J. Dumarchez¹³, B. Epp²³, S. Falciano¹⁴,
C. Fernandez⁴, C. Fisher¹⁵, Y. Fisyak¹⁷, F. Fontanelli⁶, J.R. Fry⁸,
S. Ganguli², U. Gasparini¹², S. Gentile¹⁴, D. Gibaut¹¹, A. Goshaw⁴,
F. Grard¹⁰, A. Gurtu², R. Hamatsu⁷, T. Handler²⁰, E.L. Hart²⁰, L. Haupt¹⁸,
S. Hellman¹⁸, J.J. Hernandez⁴, S.O. Holmgren¹⁸, M.A. Houlden⁸,
J. Hrubec²³, P. Hughes¹⁵, D. Huss¹⁹, Y. Iga⁷, M. Iori¹⁴, E. Jegham¹⁹,
E. Johanson¹⁸, I. Josa⁹, J. Kesteman¹⁰, E. Kistenev¹⁷, I. Kita⁷,
S. Kitamura⁷, V. Kniazev¹⁷, D. Kuhn²³, M. Laloum⁵, J. Lemonne³, H. Leutz⁴,
L. Lyons¹¹, M. MacDermott¹⁵, P.K. Malhotra², F. Marchetto²¹, P. Mason⁸,
M. Mazzucato¹², M.E. Michalon-Mentzer¹⁹, A. Michalon¹⁹, T. Moa¹⁸,
R. Monge⁶, L. Montanet⁴, G. Neuhofer²³, H.K. Nguyen¹³, S. Nilsson¹⁸,
H. Nowak⁴, N. Oshima⁷, G. Otter¹, J. Panella¹¹, G.D. Patel⁸,
M. Pernicka²³, P. Pilette¹⁰, C. Pinori¹², G. Piredda¹⁴, R. Plano¹⁶,
A. Poppleton⁴, P. Poropat²², R. Ragharan², S. Reucroft⁴, K. Roberts⁸,
H. Rohringer²³, A. Roth¹, J. Salicio⁹, R. Schulte¹, B. Sellden¹⁸,
M. Sessa²², K. Shankar², S. Squarcia⁶, P. Stamer¹⁶, V. Stopchenko¹⁷,
W. Struczinski¹, A. Subramanian², K. Sudhakar², M.C. Touboul¹³,
U. Trevisan⁶, C. Troncon²², T. Tsurugai⁷, V. Uvarov¹⁷, L. Ventura¹²,
P. Vilain³, E. Vlasov¹⁷, C. Voltolini¹⁹, B. Vonck³, B.M. Whyman⁸,
J. Wickens³, P. Wright¹¹, T. Yamagata⁷ and G. Zumerle¹²

Submitted to Zeitschrift für Physik C

For the respective addresses see next page.

- 1 III. Physikalisches. Inst. der Technischen Hochschule, D-5100 Aachen, Federal Republic of Germany.
- 2 Tata Institute of Fundamental Research, Bombay 400 005, India.
- 3 Vrije Univ. Brussel (VUB), B-1050 Brussel, Belgium.
- 4 CERN, European Organisation for Nuclear Research, CH-1211 Geneva 23, Switzerland.
- 5 Lab. de Physique Corpusculaire, Collège de France, F-75231 Paris Cedex 05, France.
- 6 Dipartimento di Fisica, Università di Genova, I-16146 Genova, Italy.
- 7 Tokyo University of Agriculture and Technology, High Energy Group, Koganei, Tokyo, and Tokyo Metropolitan University, Tokyo 158, Japan.
- 8 Oliver Lodge Lab., University of Liverpool, GB-Liverpool L69 3BX, England.
- 9 Grupo de Altas Energias, Junta de Energia Nuclear, E-Madrid 3, Spain.
- 10 Physique des Particules Élémentaires, Université de l'Etat à Mons, B-7000 Mons, Belgique.
- 11 Nuclear Physics Laboratory, University of Oxford, GB-Oxford OX1 3RH, England.
- 12 Dipartimento di Fisica, Università di Padova, I-35131 Padova, Italy.
- 13 Lab. de Physique Nucléaire et des Hautes Energies, Univ. Pierre et Marie Curie, F-75231 Paris Cedex 05, France.
- 14 Dipartimento di Fisica Università di Roma, "La Sapienza", I-00185 Roma, Italy.
- 15 Rutherford and Appleton Laboratory, Chilton, GB-Didcot, OX11 0QX, England.
- 16 Rutgers University, Department of Physics, New Brunswick, NJ-08903, USA.
- 17 Institut for High Energy Physics, Serpukhov, 142284 Protvino, USSR.
- 18 Institut of Physics, University of Stockholm, S-113 46 Stockholm, Sweden.
- 19 Division des Hautes Energies CRN Strasbourg and Université Louis Pasteur, B.P. 20, F-67037 Strasbourg Cedex, France.
- 20 University of Tennessee, Department of Physics and Astronomy, Knoxville, TN-37916, USA.
- 21 Istituto di Fisica, Università di Torino, I-10125 Torino, Italy.
- 22 Istituto di Fisica, Università di Trieste, I-34100 Trieste, Italy.
- 23 Institut für Hochenergiephysik der Oesterreichischen Akademie der Wissenschaften, A-1050 Wien, Austria.

ABSTRACT

D-meson lifetimes have been determined from decays observed in an exposure of the high resolution hydrogen bubble chamber LEBC in association with the European Hybrid Spectrometer (EHS) to an incident 360 GeV π^- beam. Various techniques for lifetime determination are presented and the results compared. A new model-independent analysis based on the distribution in transverse decay length is introduced and preferred over other techniques. Best values are found to be:

$$\tau(D^0) = (4.1^{+0.7}_{-0.6}) \times 10^{-13} \text{ s} \quad (60 \text{ decays})$$

$$\tau(D^\pm) = (10.7^{+2.8}_{-1.8}) \times 10^{-13} \text{ s} \quad (40 \text{ decays}).$$

The lifetime ratio is:

$$R = \frac{\tau(D^\pm)}{\tau(D^0)} = 2.6^{+0.8}_{-0.6}.$$

1. INTRODUCTION

The decay of a charm particle can be described in the spectator model by the diagram of fig. 1(a). A Cabibbo-favoured decay is shown; similar diagrams can be drawn for Cabibbo-unfavoured decay modes. Comparing this diagram to the muon decay diagram of fig. 1(b) and neglecting generation mixing effects, results in the prediction of equal lifetimes for all charm particles, given by

$$\tau(c) \approx \frac{1}{5} \left(\frac{m_\mu}{m_c} \right)^5 \tau(\mu)$$

where m_μ and $\tau(\mu)$ are the mass and lifetime of the μ -meson and m_c is the mass of the charm quark. With the accepted value of the c-quark mass, $\tau(c) \sim 5 \cdot 10^{-13}$ s.

It has been clear for sometime, however, that the lifetime of the charm D^\pm is significantly higher than that of the D^0 meson^(*). Various mechanisms have been proposed to explain this difference, particularly the presence of a non-spectator diagram in which the light quark takes part in the decay. Annihilation diagrams (fig. 1(c)) and W-exchange diagrams (fig. 1(d)) are possible for charged and neutral meson decays respectively.

Early calculations discounted the contribution from the non-spectator diagrams because of helicity conservation; however, this helicity suppression can be overcome by taking into account either gluon emission by one of the quarks or intrinsic gluons already present in the wave function of the initial state. Since in the non-spectator picture the D^\pm annihilation diagram is Cabibbo-suppressed, the charged D-meson is expected to have a lifetime longer than that of the D^0 , F^\pm and Λ_c . In addition to these diagrams, final state interactions and Pauli principle interference effects are expected to contribute.

A review of the current situation is given in [1]. A precise determination of the D^\pm and D^0 lifetimes is fundamental to the understanding of the charm particle decay mechanisms.

(*) We write D^0 for D^0/\bar{D}^0 throughout this paper.

The NA27 π^-p experiment [2] has observed a sample of 100 neutral and 83 charged charm particle decays. We have previously reported [2,3] values for the D^0 and D^\pm lifetimes based on kinematically fitted samples of 11 D^0 decaying into 4 charged particles and 20 D^\pm decaying into 3 or 5 charged particles. Kinematic fits have the advantage that the charm particle momenta, and hence individual proper lifetimes, are precisely determined. A considerable improvement in the statistical precision is clearly possible, however, if decays known to be D mesons, but with kinematically unconstrained final states, can be used. Moreover, any systematic bias that may exist because of the selection procedures for accepting kinematic fits will also be reduced when a more complete sample of charm decays is used. In this paper we discuss the techniques available for lifetime determination using larger samples of decays, whether kinematically fitted or not, and extract best values for the D^0 and D^\pm lifetimes from our data.

Several techniques have been developed to make use of unfitted decays to derive lifetime estimates. In the momentum estimator technique introduced by Franek [4] and extended in this paper, the momentum of an unfitted decay is estimated from measurements of the effective mass and momenta of the charged decay products. The impact parameter technique [5] allows the lifetime to be estimated from the distribution of the distance of closest approach (impact parameter) of the decay product tracks projected to the production vertex (fig. 2(a)). In both cases lifetimes are inferred from the distributions of measured quantities using Monte-Carlo methods.

In this paper we introduce a new technique based on the study of the distribution in transverse decay length [6]. This technique allows us to use the full event sample without model dependent Monte-Carlo assumptions. Biases, which depend on the decay topology or kinematic fitting procedures, do not affect the result. Any subset of the data selected in terms of decay kinematics, fit or no fit, can be treated independently, thereby allowing direct comparison with the results of other techniques, including kinematic fitting. We employ transverse length, in addition to the momentum estimator and impact parameter techniques, to study different, but overlapping, samples of the events. The results are compared, and the best overall values of τ_{D^0} and τ_{D^\pm} are determined.

We attach particular importance to the fact that the experiment was performed using a hydrogen bubble chamber with excellent vertex resolution, precision and picture quality. This allows the selection of a sample of decays which are unambiguously charm without the need for a full kinematic fit. The selection procedures applied to achieve this sample are described in sect. 2.

2. THE EXPERIMENTAL DATA

Data were collected using the high resolution hydrogen bubble chamber LEBC in association with the European Hybrid Spectrometer exposed at the CERN SPS to a 360 GeV/c π^- beam. Details of the experimental set up and the full data reduction system are given in [2]. A previous experiment, NA16 [7], using a prototype version of both the EHS and the bubble chamber, reported lifetimes which are in agreement with the now currently accepted values. The data reported here differ from NA16 in several important respects: the bubble chamber has improved optical resolution ($\leq 20 \mu\text{m}$) (and hence improved sensitivity to short lived decays), the spectrometer includes the ionisation sampling drift chamber ISIS [8] for particle identification, and a higher sensitivity ($15.8 \pm 0.8 \text{ events}/\mu\text{b}$) was obtained. These factors increase the quality and number of charm decay events available, and thus allow an improved determination of the lifetimes.

The film was subjected to two independent scans followed by a comparison check scan, each carefully controlled by a physicist. Events were passed for measurement if there was any evidence for a secondary decay within the charm scanning box defined in fig. 2(b). Evidence for secondary decay activity at the scanning stage was usually the observation of one or more tracks which did not point back to the main event vertex and therefore had a detectable impact parameter on either view (≥ 1 bubble diameter). A first measurement removed strange particle decays by fitting to two body channels. Charm decay candidates were required to have at least one decay track with $p_T > 250 \text{ MeV}/c$ with respect to the parent or to have a charm topology (four or more charged prongs from a neutral decay, three or more from a charged decay). Events satisfying these conditions were passed to the HPD machine for precise measurement.

The HPD measurement output of a typical event containing a pair of charm decay vertices is shown in fig. 3. The centre of each bubble is measured with a precision of $\sim 5 \mu\text{m}$ resulting in r.m.s. residuals, after fitting to a straight line, of $1.8 \mu\text{m}$ for approximately 25 master points per track. This is important for the unambiguous assignment of decay topologies and the precise determination of track impact parameters. In fig. 4 we show the measured impact parameter^(*) distribution of tracks arising directly from the production vertex with no evidence of decay. The mean "impact parameter" for these tracks is $2.5 \mu\text{m}$ which is a direct measure of the error on impact parameter following the HPD measurement and reconstruction procedure. In fig. 5 we show the impact parameter distribution for all tracks arising from charm decays after the HPD measurement. The hatched region represents those tracks added to the decays following the HPD measurement and not correctly assigned or detected at the scanning stage. Between $10 \mu\text{m}$ and $30 \mu\text{m}$ a substantial number of tracks are found after HPD measurement, however very few new tracks are found with impact parameters greater than $50 \mu\text{m}$. We conclude, therefore, that the initial scanning was very efficient in finding decays with at least one track having impact parameter $y > 50 \mu\text{m}$. Similarly, the HPD is very efficient in finding all tracks with impact parameter $> 7 \mu\text{m}$ (3σ where σ is the HPD measurement error on impact parameter).

For each decay we define (in space) the quantities l , l_{\min} , l_{\max} , l_T where: l is the observed decay length, l_{\min} is the minimum detectable decay length, l_{\max} is the maximum detectable decay length and l_T is the transverse decay length ($l_T = l \sin \theta_p$ where θ_p is the production angle). The minimum and maximum decay lengths l_{\min} , l_{\max} for a given decay are defined as follows:

l_{\min} is the length necessary to detect, with efficiency close to 1, that a decay track does not originate from the primary vertex. It is the maximum of two lengths determined by "translating" the observed decay topology along the line-of-flight of the charm particle until the maximum

(*) The impact parameter of a track is defined as the larger of the values measured in projection on the two bubble chamber views.

impact parameter of the decay tracks, y_{\max} , reduces to 50 μm on either view (approximately 2.5 resolved bubble diameters) or until the minimum impact parameter, y_{\min} , reduces to 7 μm .

l_{\max} is computed from the position of the primary vertex in the chamber, the finite length of the chamber (decays are required to occur not less than 2 cm from the end of the chamber to ensure adequate visibility and measurable track length), the depth of focus of the optical system (± 2 mm) and the boundaries of the "charm box" (see fig. 2(b)). The "charm box" is defined as a cylinder of radius 2 mm in space around the beam direction for C3, V4 and V5 decays and radius 1 mm for C1, V2 decays; (see below for definition of topology labels).

The event sample from the π^- exposure consists of 114 interactions containing visible charm decays, 69 of which have an observed charm pair, giving a total of 100 neutral and 83 charged decays. The charged and neutral decays are classified as Cn and Vn respectively, where n denotes the number of charged decay products. The sample can be subdivided into 28 C1, 78 V2, 51 C3, 22 V4 and 4 C5. For the decays used in the lifetime analysis we required that at least one decay track is hybridised, i.e. momentum well reconstructed in the spectrometer. The V4 and C5 decays are accepted as charm on the basis of topology alone, whilst for other topologies additional constraints are imposed to avoid any possible contamination:

- (a) A V2 decay is accepted as charm if at least one decay track has a transverse momentum with respect to the line of flight of the parent, $p_T > 250$ MeV/c and it is paired with a second charm decay.
- (b) A C3 decay is accepted as charm if a decay track has $p_T > 250$ MeV/c or it is paired with a second charm decay.
- (c) C1 decays are not used in the lifetime analysis. However, if the decay track has $p_T > 250$ MeV/c a C1 can complete a charm pair.

Backgrounds to these topologies arising from secondary interactions in the hydrogen are negligible, due to the visibility of the additional "charge conserving track" under high resolution. A Monte-Carlo study of

the secondary interaction background indicated < 0.3 events in the sample at the scanning stage.

In table 1 we present the sample of events satisfying all of the above conditions and the subsamples^(*) used by the four techniques discussed in the remainder of this paper.

TABLE 1

	Topology	Original Sample	Sample for τ analysis	Subsamples used by technique			
				Kin. fits	L trans.	P est	$\langle y \rangle$
D^0	V2	78	36	10	36	24	36
	V4	22	21	11	21	12	21
D^\pm	C1	28	-	-	-	-	-
	C3	48	33	17	33	17	33
	C5	4	3	3	3	3	-

The samples are highly correlated since the same events can be used by several techniques. It is valuable to compare the results obtained using the various techniques since they are sensitive to different lifetime-dependent features of the events. Statistical fluctuations which can distort one distribution may not affect another. For example, a decay having an unusually high production p_T will in consequence have a large transverse length, but will not necessarily have large impact parameters or large "estimated" longitudinal momentum.

To obtain best values for the lifetimes we take only the transverse length result for the non-fitted decays in combination with the maximum likelihood lifetime fit to the kinematically fitted decays. These are independent samples which can be simply combined.

To understand the sensitivity of the methods to statistical fluctuations in the data, and to the parameters of each method itself, we have performed an extensive Monte-Carlo study. This consists of generating 500 equivalent NA27 "experiments" according to the best data

(*) For the kinematic fit sample, the definition of l_{\min} is that of ref. [2], EXCEPT where comparison is made with other lifetime techniques, using the same data sample, when the definition discussed above is used throughout.

available for production and decay characteristics. D mesons were generated according to the x_F and p_T^2 distributions, determined by this experiment, of $(1 - |x_F|)^{3.5}$ (one component fit) and $\exp(-1.18 p_T^2)$ respectively [9]. These decayed, with mean lifetimes of 3.5×10^{-13} s and 9.85×10^{-13} s for neutral and charged mesons, respectively, into channels determined by the known branching ratios, according to simple phase space. The relevant cuts for spectrometer acceptance were imposed. Cuts appropriate to the selection criteria for each method were applied to the events, and an event sample generated having the same numbers of events in each of the sub-channels, for each method, as we have in the experiment (table 1). The above process was repeated to give 500 such Monte-Carlo data samples. The results of this simulation for each method are reported in the appropriate sections.

The charged charm sample selected could in principle include decays other than D^\pm , such as F^\pm or Λ_c^\pm . An attempt to extract a Λ_c or F signal at short lifetimes will be reported in a later paper. Here we note that with the event selection defined above, the indirect techniques give a charged lifetime which is stable against variation of impact parameter cuts i.e. within the selected sample we have no evidence of a short lived component. No unambiguous F fits were observed in the experiment [10]. Three probable Λ_c decays were observed [2] however these are excluded from the following analysis.

3. LIFETIME DETERMINATIONS

3.1 Lifetimes from constrained kinematic fits

This method is direct and without model dependent parameters. However, because of the need for a well determined momentum, and hence a unique kinematic fit for each decay, only a small sample of all decays can be used. For each decay the proper lifetime t^i is obtained from the measured decay length and fitted momentum. The minimum and maximum detectable proper lifetimes t_{\min}^i , t_{\max}^i are determined from the corresponding decay lengths l_{\min}^i and l_{\max}^i as defined in sect. 2. In the present data a sample of 20 charged decays, and 21 neutral decays (11 V4 and 10 V2) satisfy these criteria.

A maximum likelihood fit was performed to these decays using the likelihood function:

$$L(\tau) = \prod_i \frac{1}{\tau} \frac{\exp(-t^i/\tau)}{\exp(-t_{\min}^i/\tau) - \exp(-t_{\max}^i/\tau)}$$

We find the following mean lifetimes where the error quoted corresponds to a fall in the log likelihood from the maximum by 0.5.

$$\tau(D^0) = 3.5^{+1.4}_{-0.9} \times 10^{-13} \text{ s} \quad (11 \text{ V4})$$

$$\tau(D^{\pm}) = 9.8^{+3.4}_{-2.2} \times 10^{-13} \text{ s} \quad (20 \text{ C3/C5}).$$

A D^0 lifetime determination based on the well constrained V2 decays yields:

$$\tau(D^0) = 3.6^{+1.5}_{-1.0} \times 10^{-13} \text{ s} \quad (10 \text{ V2})$$

and using the combined V2 + V4, D^0 sample we obtain:

$$\tau(D^0) = 3.6^{+1.0}_{-0.7} \times 10^{-13} \text{ s} \quad (21 \text{ decays}).$$

The ratio of lifetimes is then:

$$R = \frac{\tau(D^{\pm})}{\tau(D^0)} = 2.7^{+1.2}_{-0.8}$$

The results of the likelihood fit are stable against variation in ℓ_{\min} .

3.2 The transverse length technique

This method uses the correlation between the transverse decay length ℓ_T (fig. 2(b)) and the lifetime:

$$\ell_T = t p_T c/m.$$

In order to derive the expected ℓ_T distribution we make use of the independence of the p_T and t distributions.

$$\frac{\partial^2 N}{\partial p_T \partial t} = \frac{1}{\tau} e^{-t/\tau} \cdot F(p_T)$$

where $F(p_T)$ is the functional form of the p_T distribution. Transforming variables to p_T , l_T we obtain

$$\frac{\partial^2 N}{\partial l_T^2 \partial p_T} = \frac{m}{p_T c \tau} \exp\left\{-\frac{m l_T}{p_T c \tau}\right\} \cdot F(p_T)$$

and the l_T distribution is found by integrating over p_T

$$\frac{dN}{dl_T} = \int_0^\infty \frac{m}{p_T c \tau} \exp\left\{-\frac{m l_T}{p_T c \tau}\right\} \cdot F(p_T) dp_T .$$

In the absence of cuts to the sample the likelihood function is given by

$$L(\tau) = \prod_i \frac{m}{c \tau} \int_0^\infty \frac{1}{p_T} \exp\left\{-\frac{m p_T^i}{p_T c \tau}\right\} F(p_T) dp_T .$$

The critical requirement is therefore $F(p_T)$, the form of the p_T distribution. In this experiment the distribution in p_T^2 is well described by a simple exponential [9]

$$\frac{dN}{dp_T^2} \propto \exp\left[-1.18 \begin{matrix} +0.18 \\ -0.16 \end{matrix} p_T^2\right]$$

with no significant difference between D^0 and D^{\pm} and in good agreement with other data. We therefore use:

$$F(p_T) \propto p_T \exp[-b p_T^2], \text{ where } b = 1.18 \begin{matrix} +0.18 \\ -0.16 \end{matrix} .$$

The integration can then be performed numerically.

As a check on the principle of the method the 500 Monte-Carlo experiments (each with 100 decays) described in sect. 2 have been studied. The distribution of D^0 lifetimes determined for each experiment using the transverse length technique is shown in fig. 6(a) whilst the actual distribution in mean lifetimes for the experiments generated is shown in fig. 6(b). The standard deviation of the distribution of "transverse length estimated" lifetimes is 0.45×10^{-13} s compared with 0.35×10^{-13} s for the actual distribution of mean lifetimes. The transverse length technique is therefore only slightly inferior for lifetime determination to the use of kinematic fits which would be expected to return the actual mean lifetimes in fig. 6(b). Note that both distributions 6(a) and 6(b) have a mean of $3.5 \cdot 10^{-13}$ s (the input to the Monte-Carlo) as expected.

For each decay in the sample there are minimum and maximum detectable transverse lengths l_{Tmin}^i, l_{Tmax}^i found by projecting l_{min}^i and l_{max}^i onto the transverse plane (the plane transverse to the beam). The effect of these cuts in the normalisation can be studied by first considering the probability of observing the event at l_T^i if p_T is fixed.

$$P(l_T^i, \tau)_{p_T} = \frac{m}{p_T c \tau} \frac{\exp\{-\frac{l_T^i m}{p_T c \tau}\}}{\exp\{-\frac{l_{Tmin}^i m}{p_T c \tau}\} - \exp\{-\frac{l_{Tmax}^i m}{p_T c \tau}\}} .$$

The probability of observing the event, in the absence of kinematic constraints among the variables (see below), would be:

$$P(l_T^i, \tau) = \int_0^\infty \frac{m}{p_T c \tau} \frac{\exp\{-\frac{l_T^i m}{p_T c \tau}\}}{\{\exp\{-\frac{l_{Tmin}^i m}{p_T c \tau}\} - \exp\{-\frac{l_{Tmax}^i m}{p_T c \tau}\}\}} \cdot F(p_T) dp_T .$$

Since $P(l_T^i, \tau)_{p_T}$ has been normalised to 1 and $\int_0^\infty F(p_T) dp_T = 1$ the likelihood function is therefore approximated as:

$$L(\tau) = \prod_i \int_0^\infty \frac{m}{p_T c \tau} \frac{\exp\{-\frac{l_T^i m}{p_T c \tau}\}}{\{\exp\{-\frac{l_{Tmin}^i m}{p_T c \tau}\} - \exp\{-\frac{l_{Tmax}^i m}{p_T c \tau}\}\}} \cdot F(p_T) dp_T .$$

A Monte-Carlo study shows that for the conditions of the experiment, this simple function returns a slight overestimate of the lifetime. The correction factor which must be applied to the result in order to return the correct (input) lifetime is shown in fig. 7.

The reason for the above correction can be understood as follows. The translation from l_{min}^i, l_{max}^i to l_{Tmin}^i, l_{Tmax}^i can only be made if θ^i , the production angle, is fixed. The normalisation derived above is however correct only if $p_L(X_F)$ is free to vary independently of p_T . This

is not so because $p_L = p_T \cot\theta^i$. At this stage we choose to correct the result of the approximated maximum likelihood estimate, using the above function, rather than to modify the function to take account rigorously of the complex normalisation. The correction factor applied is small and insensitive to the form of the production distribution.

Fig. 8 shows the experimental distributions of $(\ell_T - \ell_{Tmin})$ with fitted curves corresponding to the lifetimes obtained below. The distributions are very different for the D^0 and D^\pm samples, with $\langle L_T - L_{Tmin} \rangle = 57 \mu\text{m}$ for D^0 decays and $130 \mu\text{m}$ for D^\pm decays which immediately shows evidence for the ratio of lifetimes ~ 2.4 . Note that the losses due to the scanning cuts on ℓ_T due to the charm box (2 mm for D^\pm and D^0 V4, 1 mm for D^0 V2) are negligible.

It is clearly important to demonstrate that the lifetime results are stable against variations in the cuts used to define the data sample. In fig. 9 we show the sensitivity of the lifetime results to the choice of ℓ_{min} . In this figure the derived lifetimes are plotted as a function of f where f is a scaling factor for ℓ_{min} . Clearly both D^0 and D^\pm lifetimes are insensitive to the exact value of the cut above ℓ_{min} . In the region $f < 1$ there are known scanning losses (decays occurring close to the primary vertex in the forward direction in complex events) leading to an apparent increase in $\tau(D^0)$. The choice of $f = 1$ (i.e. $y_{max} > 50 \mu\text{m}$, $y_{min} > 7 \mu\text{m}$) is clearly reasonable. In fig. 10 we show the derived lifetimes only as a function of the cut on y_{max} . No losses are apparent and representative values are chosen to avoid fluctuations due to individual events.

The statistical uncertainty in the parameter "b" is reflected in the statistical error on τ . Fig. 11 shows that the results are not too sensitive to systematic errors in "b", for example, a 10% systematic change in the value of b would lead to a 5% change in lifetimes.

Our final values for the lifetimes using this technique are therefore

$$\tau(D^0) = (4.8^{+1.1}_{-1.0}) \times 10^{-13} \text{ s} \quad (36 \text{ V2})$$

$$\tau(D^0) = (3.8^{+1.3}_{-0.9}) \times 10^{-13} \text{ s} \quad (21 \text{ V4})$$

$$\tau(D^0) = (4.5^{+0.8}_{-0.7}) \times 10^{-13} \text{ s} \quad (57 \text{ V2/V4 decays})$$

$$\tau(D^\pm) = (10.4^{+2.8}_{-2.0}) \times 10^{-13} \text{ s} \quad (36 \text{ C3/C5 decays}).$$

The ratio of lifetimes R is given by

$$R = \frac{\tau(D^\pm)}{\tau(D^0)} = 2.3^{+1.0}_{-0.7} .$$

As an additional check we apply the transverse length technique to the sample of 20 fitted charged decays studied by the simple maximum likelihood technique in sect. 3.1. We find $\tau(D^\pm) = (9.8^{+3.7}_{-2.5}) \times 10^{-13} \text{ s}$ compared with the value of $(9.8^{+3.4}_{-2.2}) \times 10^{-13} \text{ s}$ obtained from the likelihood fit to the measured proper time distribution.

Finally we apply the technique to the no fit data sample i.e. excluding the 20 fitted D^\pm and 21 fitted D^0 V2/V4 decays^(*). We find:

$$\tau(D^0) = (4.7^{+1.1}_{-0.9}) \times 10^{-13} \text{ s} \quad (39 \text{ V2/V4 no fits})$$

$$\tau(D^\pm) = (12.9^{+5.1}_{-3.4}) \times 10^{-13} \text{ s} \quad (20 \text{ C3/C5 no fits}) .$$

3.3 The momentum estimator technique

In this method an estimate of each charm particle momentum is obtained for decays without a kinematic fit. The technique, originally proposed by Franek [4], consists of finding a simple scaling law to estimate the D-meson momentum (p_{est})

$$p_{\text{est}} = \alpha \frac{M_D p_{\text{vis}}}{M_\pi}$$

(*) Note that only 16 of the fitted charged decays and 18 of the fitted neutral decays survive the selection criteria of sect. 2.

where p_{vis} is the observed momentum of the charged decay products and M_{vis}^π is their effective mass assuming that they are all pions. The parameter α is determined by Monte-Carlo as described below. The method does not require knowledge of the presence or identity of any neutral particles and has been extended to allow more general application to higher energy experiments [11]. In particular, to determine the lifetimes using the likelihood method, we will not simply use the scaling law mentioned above, but we will take into account the distribution $dN/d\alpha$ as given by Monte-Carlo calculations.

The form of the scaling law is obtained by considering the transformation from the D-meson rest frame to the laboratory

$$P_{vis} = \frac{E_D}{M_D} P_{vis}^{rest} \cos\theta^* + \frac{P_D}{M_D} E_{vis}^{rest}$$

where E_D , P_D , M_D refer to the energy, momentum and mass of the D meson in the lab frame, $P_{vis}^{rest} \cos\theta^*$ and E_{vis}^{rest} are the longitudinal momentum and energy of the charged decay products transformed to the D meson rest frame. P_{vis} is the longitudinal momentum (along the D meson direction) in the laboratory.

If we consider only decays such that $x_F(D) > 0$ then the acceptance of the NA27 spectrometer is $\sim 95\%$ for all charged decay products and we can write

$$\langle P_{vis} \rangle \sim \frac{P_D}{M_D} \langle E_{vis}^{rest} \rangle .$$

Typically $P_{vis}^{rest} \ll M_{vis}$ for D decays so that $E_{vis}^{rest} = \gamma M_{vis}$ with $\gamma \sim 1$ (M_{vis} is the invariant mass of the hybridized charged particles within the spectrometer acceptance). One then has:

$$\langle P_{vis} \rangle = \gamma \frac{P_D}{M_D} M_{vis} .$$

The difference between M_{vis} and M_D , and correspondingly P_{vis} and p_D , arises from the presence in the final state of neutral particles and non-hybridized charged particles. The identity of charged particles is not known with complete reliability. However, two variables are known unambiguously for each event, namely P_{vis} and M_{vis}^π , where the latter is

the invariant mass assuming all relevant charged particles are pions. Putting $M_{\text{vis}} = KM_{\text{vis}}^{\pi}$ ($K \sim 1$) we can write the scaling relationship

$$P_{\text{est}} = \alpha \frac{M_D P_{\text{vis}}}{M_{\text{vis}}^{\pi}}$$

The dependence of the scaling factor α on the values of M_{vis}^{π} and P_{vis} is determined by Monte-Carlo simulation, using the expression

$$\alpha = \frac{M_{\text{vis}}^{\pi} P_{\text{true}}}{M_D P_{\text{vis}}}$$

where P_{true} is the momentum of a particular (Monte-Carlo generated) D meson. There is no one-to-one correspondence between p_{true} and $p_{\text{vis}}/M_{\text{vis}}^{\pi}$, since the derivation of the scaling law involves averaging over the relevant quantities. Therefore, the scaling parameter α has a distribution, the shape of which is a function of the parameters M_{vis}^{π} and p_{vis} . The probability distributions $dN/d\alpha$ were determined by Monte-Carlo for the values $(M_{\text{vis}}^{\pi}, p_{\text{vis}})$ in intervals of $50 \text{ MeV}/c^2$ by $20 \text{ GeV}/c$ covering the physical region. The distributions in α were determined for each decay topology separately.

Fig. 12(a) shows the distribution of α^{-1} (for $1/p_{\text{est}}$ and hence t_{est}) as a function of M_{vis}^{π} averaged over p_{vis} , for the C3 topology. Fig. 12(b) shows the corresponding distribution as a function of p_{vis} averaged over M_{vis}^{π} . The broad distribution in α^{-1} at small values of M_{vis}^{π} and p_{vis} corresponds to a poor estimation of the lifetime, while the narrow distributions at large values of M_{vis}^{π} and p_{vis} represent good lifetime estimates. A full discussion is given in [11]. The distributions in α^{-1} are appreciably narrower for the V4 and C5 topologies, and slightly broader for the V2 topology. Fig. 13 shows for the C3 topology the ratio of the mean values $\langle t_{\text{est}} \rangle$ and $\langle t_{\text{true}} \rangle$ calculated for 500 Monte-Carlo experiments as discussed in sect. 2. The results of the Monte-Carlo study are insensitive to the detailed parametrization in x_F and p_T^2 of the D-meson production. We conclude that the estimator technique can confidently be used to analyze the data for this experiment.

In order to apply the method to the data sample, cuts must be applied in addition to those used to define the full sample. We require (a) at least two tracks with well determined momenta in the spectrometer and (b) a cut is applied to P_{est} such that $x_F(\text{estimated}) > 0$ for all events. This x_F cut was imposed by using the $\langle \alpha \rangle$ corresponding to the α -distribution of the particular values p_{vis}^i and $(M_{vis}^\pi)^i$ in order to obtain a unique value x_F^{est} for each decay. The drift of events across the $x_F = 0$ boundary was investigated by Monte-Carlo, and found to be $\sim 0.4\%$. The data sample available to the estimator technique reduces to 36 D^0 (24 V2 and 12 V4) and 20 D^\pm (17 C3 + 3 C5).

For the lifetime determination the distribution of p_{est} for each event was used as derived from $dN/d\alpha$ at the appropriate M_{vis}^π and p_{vis} .

The normalised likelihood function is then written:

$$L(\tau) = \prod_i \frac{\int_0^\infty \frac{1}{\lambda^i(\alpha)} \exp\{-\ell^i/\lambda^i(\alpha)\} f^i(\alpha) d\alpha}{\int_0^\infty \left[\exp\left[-\frac{\ell_{min}^i}{\lambda^i(\alpha)}\right] - \exp\left[-\frac{\ell_{max}^i}{\lambda^i(\alpha)}\right] \right] f^i(\alpha) d\alpha}$$

where $f^i(\alpha) = dN/d\alpha$ and $\lambda^i(\alpha) = \alpha p_{vis}^i c\tau / (M_{vis}^\pi)^i$. The integrals are evaluated numerically.

The lifetimes obtained using this method are:

$$\tau(D^0) = 4.8^{+1.4}_{-1.0} \times 10^{-13} \text{ s} \quad (24 \text{ V2})$$

$$\tau(D^0) = 3.7^{+1.5}_{-0.9} \times 10^{-13} \text{ s} \quad (12 \text{ V4})$$

$$\tau(D^0) = 4.4^{+1.0}_{-0.7} \times 10^{-13} \text{ s} \quad (36 \text{ V2/V4})$$

$$\tau(D^\pm) = 11.5^{+4.5}_{-2.8} \times 10^{-13} \text{ s} \quad (17 \text{ C3} + 3 \text{ C5})$$

$$R = \frac{\tau(D^\pm)}{\tau(D^0)} = 2.6^{+1.2}_{-0.8}$$

3.4 The impact parameter method

The impact parameter distribution of charged decay products taken with respect to the production vertex (fig. 2(a)) can be used to determine the D-meson lifetime [5]. For a particular decay track the impact parameter can be written:

$$y = L \sin \theta_{\text{decay}} = \frac{p \cdot ct}{m} \cdot \sin \theta_{\text{decay}}$$

where L is the D-meson decay length, θ_{decay} is the angle of the decay track to the D-meson direction and p is the D-meson momentum, all projected onto the film plane. To a good approximation the impact parameter y is independent of the D-meson momentum p, since $\sin \theta_{\text{decay}}$ varies as 1/p. In the absence of cuts on the data, the average impact parameter is proportional to the mean lifetime, $\langle y \rangle \propto \tau$.

To evaluate the dependence of $\langle y \rangle$ on τ we have studied events generated by the Monte-Carlo procedure which have varying input lifetimes. Since y is nearly independent of the D meson momentum, the results are insensitive to the production variables x_F and p_T : the distribution in y depends only on the D-lifetime and the decay dynamics. The dependence of $\langle y \rangle$ on τ is shown in fig. 14. The systematic error, coming from uncertainty in the branching ratios, is small compared with the statistical errors. The measured mean impact parameters are 148 μm for the V2 topology, 93 μm for the V4 topology and 229 μm for the C3 topology.

The distributions in the measured impact parameters, together with the appropriate curves for the lifetimes given below, are shown in fig. 15. In fig. 16 we show the derived lifetimes as a function of the impact parameter cut, y_{max} . The lifetimes are stable indicating that the result is insensitive to the precise value of the cut. We find:

$$\tau(D^0) = (5.6^{+1.7}_{-1.2}) \times 10^{-13} \text{ s} \quad (36 \text{ V2})$$

$$\tau(D^0) = (3.4^{+1.2}_{-0.7}) \times 10^{-13} \text{ s} \quad (21 \text{ V4})$$

$$\tau(D^0) = (4.6^{+1.0}_{-0.7}) \times 10^{-13} \text{ s} \quad (57 \text{ V2 and V4})$$

$$\tau(D^\pm) = (11.9^{+3.9}_{-2.6}) \times 10^{-13} \text{ s} \quad (33 \text{ C3})$$

$$R = \tau(D^\pm)/\tau(D^0) = 2.6^{+1.0}_{-0.7}$$

Inspection of the distributions given in fig. 14 shows that the C3 and V4 distributions are well fitted by the Monte-Carlo for the appropriate lifetimes. We note that there is a V2 charm decay (not uniquely fitted) which is relatively long lived and contributes to the tail of the V2 impact parameter distribution and hence raises the mean $\langle y \rangle$. We discuss this event and the question of anomalous long-lived D^0 's in sect. 4.

4. COMPARISON OF RESULTS

The transverse length technique is model independent and uses the full statistics available for the lifetime analysis. We therefore prefer this technique for the treatment of unfitted decays. To establish confidence in the method we consider first the result of applying the analysis to the kinematic fit sample. The results are given in row 2 of table 2. Row 1 gives the lifetimes derived from the fitted sample in the usual way (sect. 3.1). Clearly the results are very consistent showing that the transverse length technique yields the expected result when applied to the subsample of fitted decays.

TABLE 2

	$\tau(D^0)$ V2	$\tau(D^0)$ V4	$\tau(D^0)$ V2 + V4	$\tau(D^\pm)$ C3 + C5	
Same Event Sample	Kinematic fits	3.6 $^{+1.5}_{-1.0}$ (10)	3.5 $^{+1.4}_{-0.9}$ (11)	3.6 $^{+1.0}_{-0.7}$ (21)	9.8 $^{+3.4}_{-2.2}$ (20)
	Transverse length fits	4.3 $^{+2.1}_{-1.3}$	3.2 $^{+1.6}_{-1.0}$	3.6 $^{+1.3}_{-0.8}$	9.8 $^{+3.7}_{-2.5}$
	Transverse length no fits	4.9 $^{+1.5}_{-1.0}$ (28)	4.1 $^{+1.9}_{-1.2}$ (11)	4.7 $^{+1.1}_{-0.9}$ (39)	12.9 $^{+5.1}_{-3.4}$ (20)

Row 3 of table 2 gives the lifetimes derived from the transverse length technique applied to those events not giving a kinematic fit. We note that the no fit sample yields a consistently larger result than the fit sample. Although this could be statistical it could also be an indication of a bias entering through the selection of events that satisfy the fitting procedure.

In table 3 we collect the results of all techniques applied to the full samples available (all lifetimes are $\times 10^{-13}$ s).

TABLE 3

Topology	fits	L Trans.	P Estimator	<y> Impact Param.
D^0 V2	3.6 $^{+1.5}_{-1.0}$	4.8 $^{+1.1}_{-1.0}$	4.8 $^{+1.4}_{-1.0}$	5.6 $^{+1.7}_{-1.2}$
D^0 V4	3.5 $^{+1.4}_{-0.9}$	3.8 $^{+1.3}_{-0.9}$	3.7 $^{+1.5}_{-0.9}$	3.4 $^{+1.2}_{-0.7}$
All D^0	3.6 $^{+1.0}_{-0.7}$	4.5 $^{+0.8}_{-0.7}$	4.4 $^{+1.0}_{-0.7}$	4.6 $^{+1.0}_{-0.7}$
D^\pm	9.8 $^{+3.4}_{-2.2}$	10.4 $^{+2.8}_{-2.0}$	11.5 $^{+4.5}_{-2.8}$	11.9 $^{+3.9}_{-2.6}$
$R = \frac{\tau(D^\pm)}{\tau(D^0)}$	2.7 $^{+1.2}_{-0.8}$	2.4 $^{+1.0}_{-0.7}$	2.6 $^{+1.2}_{-0.8}$	2.6 $^{+1.0}_{-0.7}$

Note that the kinematic fit sample used to contribute to the final result includes an additional 3 constrained D^0 and 4 constrained D^\pm decays allowed by the minimum length criterion of ref. [2].

We quote as our final result the values for $\tau(D^0)$ and $\tau(D^\pm)$ using a combination of the fits, where available, and the transverse length applied to the no-fits. We obtain:

$$\tau(D^0) = (4.1 \text{ }^{+0.7}_{-0.6}) \times 10^{-13} \text{ s (60 V2/V4 decays)}$$

$$\tau(D^\pm) = (10.7 \text{ }^{+2.8}_{-1.8}) \times 10^{-13} \text{ s (40 C3/C5 decays)}$$

$$R = \frac{\tau(D^\pm)}{\tau(D^0)} = 2.6 \text{ }^{+0.8}_{-0.6} .$$

The indirect techniques operating on the same data sample are very consistent. However, the V2 decays all yield a larger lifetime than the V4 decays. The rigorous selection procedure applied ensures the absence of non-charm background in the V2 sample. One decay, however, seems to contribute significantly to the indirect V2 result. It does not give a good kinematic fit but is clearly long lived. The total energy balance for the event and possible OC fit solutions indicate a lifetime in the range $17-30 \times 10^{-13}$ s. The decay length is 6 cm. For a mean lifetime of 4.1×10^{-13} s we would expect 0.6 events in our sample with $t > 20 \times 10^{-13}$ s. This event is therefore consistent with the overall lifetime of 4.1×10^{-13} s.

5. CONCLUSIONS

In conclusion we re-emphasize the clean nature of the experiment:

- The hydrogen bubble chamber ensures negligible background from secondary interactions.
- The absence of a charm trigger removes any possible bias in the data taking.
- The high resolution optical system ensures high detection efficiency for charm decay vertices at the scanning stage.
- The high precision of the HPD measurement ensures that tracks and vertices are correctly related.
- The cuts applied to the data sample remove all background from strange particle decays and ensure lifetime independent detection efficiency.

Four techniques for lifetime determination have been studied, three of which allow the use of unfitted decays. Very consistent results are obtained using the indirect techniques. The number of unambiguous fits obtained and used in the fit sample is at the level expected from the known branching ratios. The transverse length technique for lifetime

determination is introduced and is preferred over other indirect methods, giving model independent results for $\tau(D^0)$ and $\tau(D^\pm)$. The results are stable against variation in the visibility cut parameters.

Best values for $\tau(D^0)$ and $\tau(D^\pm)$ are derived using a combination of the fits, where available, and the transverse length technique applied to the no-fits. We obtain:

$$\tau(D^0) = (4.1^{+0.7}_{-0.6}) \times 10^{-13} \text{ s (60 V2/V4 decays)}$$

$$\tau(D^\pm) = (10.7^{+2.8}_{-1.8}) \times 10^{-13} \text{ s (40 C3/C5 decays)}$$

$$R = \frac{\tau(D^\pm)}{\tau(D^0)} = 2.6^{+0.8}_{-0.6} .$$

The experiment does not show any evidence for long-lived D^0 's. We note that the V4 decay reported by the SHF Collaboration [12] with lifetime $\sim 55 \times 10^{-13}$ s remains anomalous.

Since the data presented in this paper represent only 30% of the full data collected by the collaboration (including a 400 GeV/c proton-proton exposure), final values for charm particle lifetimes will appear in a forthcoming publication.

Acknowledgements

This study has been made possible by the excellent quality of the high resolution pictures obtained from LEBC and the careful work of the scanning teams. We would therefore like to thank particularly the engineers and applied physicists involved in the design and operation of the bubble chamber and the scanning staff at the various laboratories of the collaboration. In addition we acknowledge the cooperation and highly competent typing work, of Mu King. We thank also the National Funding agencies for supporting this work.

REFERENCES

- [1] See for example, C. Caso and M.C. Touboul, CERN/EP 85-176. To be published in La rivista del Nuovo Cimento.
- [2] M. Aguilar-Benitez et al., Zeitschr. Phys. C31 (1986) 491.
- [3] M. Aguilar-Benitez et al., Phys. Lett. 146B, 3 (1984) 266.
- [4] B. Franek, Rutherford Appleton Laboratory Report RAL 85-026 (1985).
- [5] S. Petrera and G. Romano: Nucl. Instr. and Meth. 174 (1980) 61.
P. Checchia et al., INFN Note INFN/PD/EHS 84.
- [6] K. Roberts, Ph.D Thesis, University of Liverpool (1986).
- [7] M. Aguilar-Benitez, Phys. Lett. 122B, (1983) 312.
- [8] W.W.M. Allison et al., Nucl. Instr. and Methods 224 (1982) 217.
- [9] M. Aguilar-Benitez et al, Phys. Lett. 161B, 4 (1985) 400.
- [10] M. Aguilar-Benitez et al., Phys. Lett. 156B (1985) 444.
- [11] D. Gibaut, D.Phil Thesis, University of Oxford (1986).
- [12] K. Abe et al., SLAC-PUB-3493 or RAL-84-110 (1984).

FIGURE CAPTIONS

- Fig. 1 (a) Spectator diagram for D meson decay. Note that decays of charm baryons will occur with similar graphs;
- (b) Sketch of the muon decay diagram;
- (c) Annihilation diagram (Cabibbo suppressed) for a D^\pm meson decay;
- (d) W-exchange diagram for a D^0 decay. In (c) and (d) the curved lines represent gluon emission.
- Fig. 2 (a) Definition of the impact parameter y . Note that y is defined in the film plane projection with unit magnification to the chamber.
- (b) Definition of the transverse length L_T , decay length L and the charm scanning box.
- Fig. 3 A typical NA27 event. The track digitizings are shown following the HPD measurement. The event has a V4 D^0 decay and a V2 D^0 decay.
- Fig. 4 Measured impact parameters for tracks originating from the main vertex. The distribution is a direct measure of the error on the impact parameter.
- Fig. 5 Impact parameter distribution for all tracks associated with charm particle decays. The hatched region represents those tracks added to the decays after the HPD measurement and therefore not detected at the scanning stage.
- Fig. 6 Results of the transverse length analysis applied to the Monte-Carlo generated experiments.
- (a) Histogram of τ_{LT} (mean lifetime per experiment) found by transverse length analysis of 500 experiments.
- (b) Histogram of τ_{true} as generated for the same 500 experiments.

FIGURE CAPTIONS (Cont'd)

- Fig. 7 Correction factor applied to results of the simple transverse length likelihood function estimate of τ as a function of τ for conditions of this experiment.
- Fig. 8 Transverse length distributions ($L_T - L_{Tmin}$); L_T is the measured transverse length and L_{Tmin} the minimum detectable transverse length for the event. The curves represent the fits to the lifetimes derived for D^0 and D^\pm using this technique.
- Fig. 9 Sensitivity of transverse length lifetime results to the choice of l_{min}^i . The parameter f is used to multiply all minimum lengths l_{min}^i . The results are insensitive to f for $f > 1.0$.
- Fig. 10 Sensitivity of the transverse length lifetime result to the choice of Y_{max} .
- Fig. 11 Sensitivity of the transverse length lifetimes to the transverse momentum parameter "b". The point indicates the value used in this analysis.
- Fig. 12 Monte-Carlo evaluation of the parameter α^{-1} , used in the momentum estimator technique for C3 D^\pm decays.
- (a) As a function of the visible mass M_{vis}^π averaged over P_{vis} .
- (b) As a function of p_{vis} averaged over M_{vis}^π .
- Fig. 13 Results of the momentum estimator analysis applied to the Monte-Carlo generated events. The ratio of the mean values $\langle t_{est} \rangle$ and $\langle t_{true} \rangle$ calculated for each of the 500 Monte-Carlo experiments each containing 100 events is shown.
- Fig. 14 Monte-Carlo result showing the dependence of mean impact parameter on lifetime for V2, V4 and C3 decays.

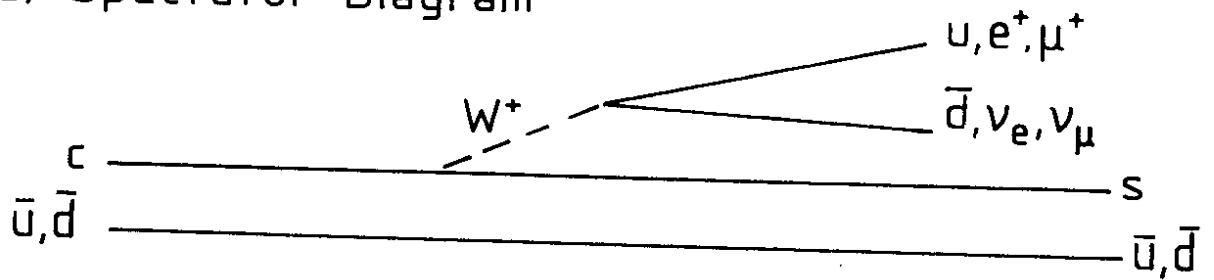
FIGURE CAPTIONS (Cont'd)

Fig. 15 Distributions of measured impact parameters. The curves represent the expected distributions for the lifetimes derived from the mean y (as in text).

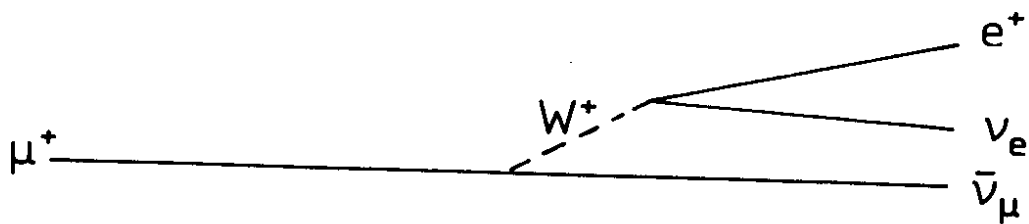
Fig. 16 Lifetime result from the impact parameter technique as a function of the y_{\max} cut.

D-MESON DECAY MECHANISMS

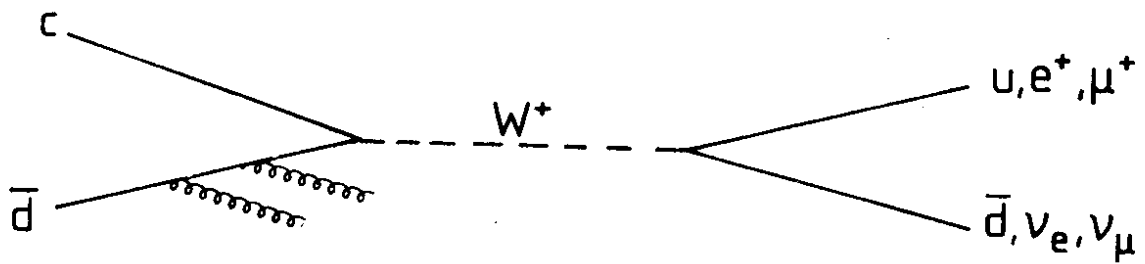
a) Spectator Diagram



b) Muon Decay



c) Annihilation Diagram.



d) Exchange Diagram

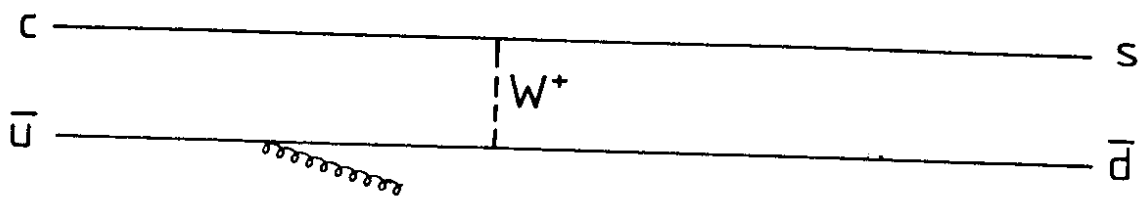
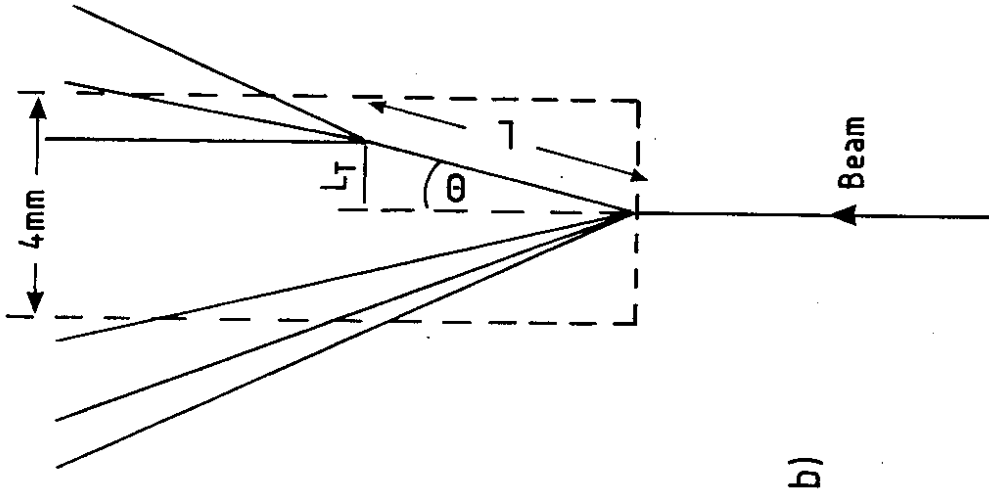
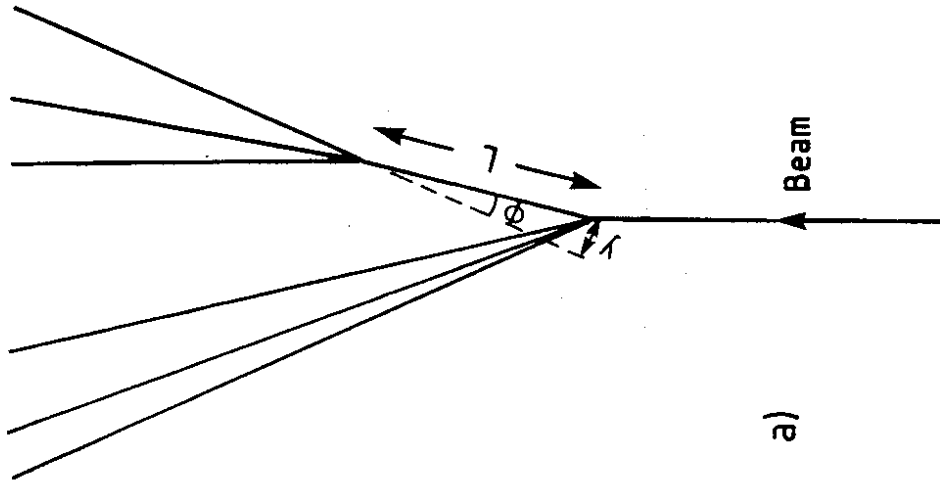


Fig. 1



b)



a)

Fig. 2

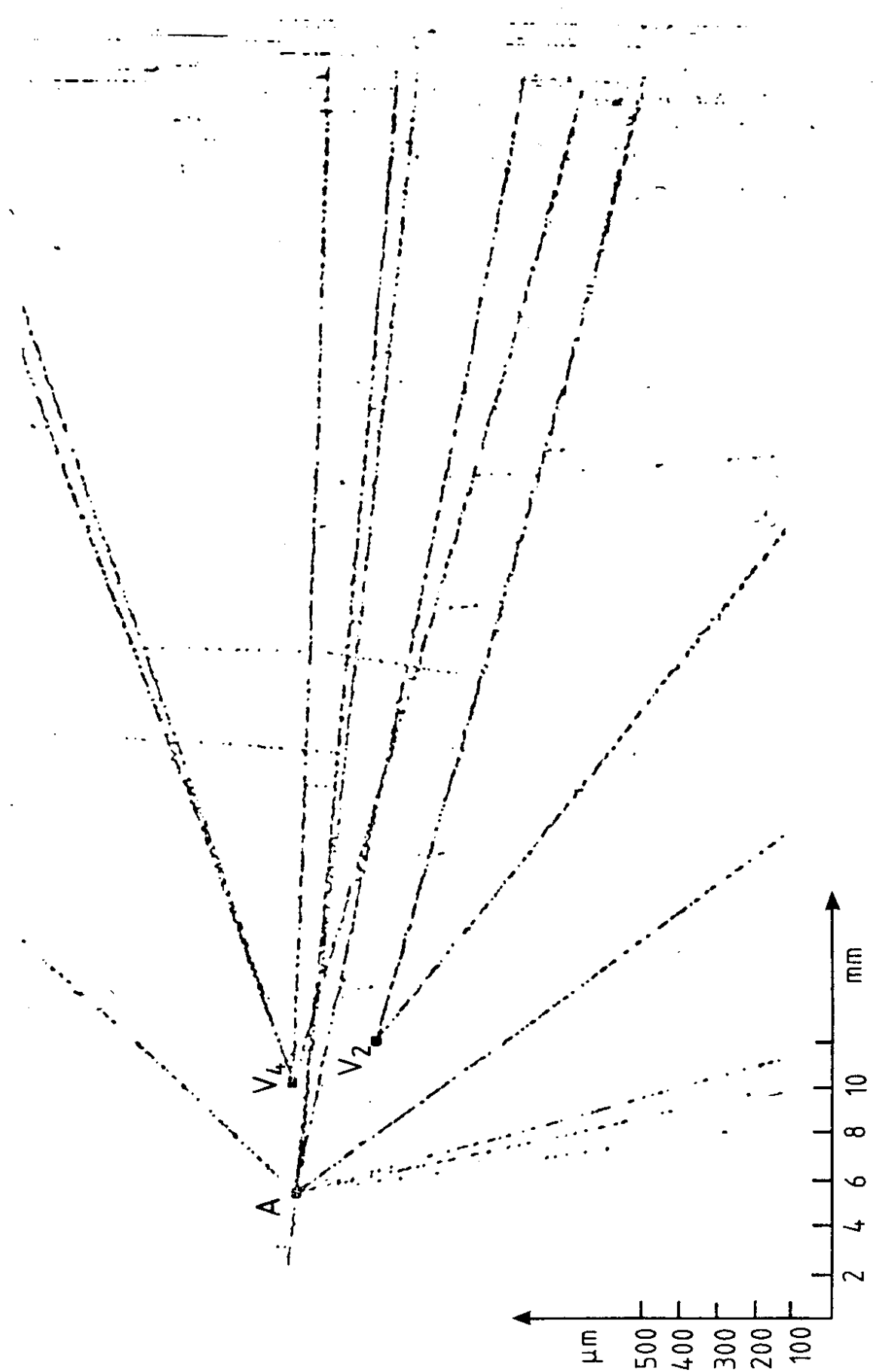


Fig. 3

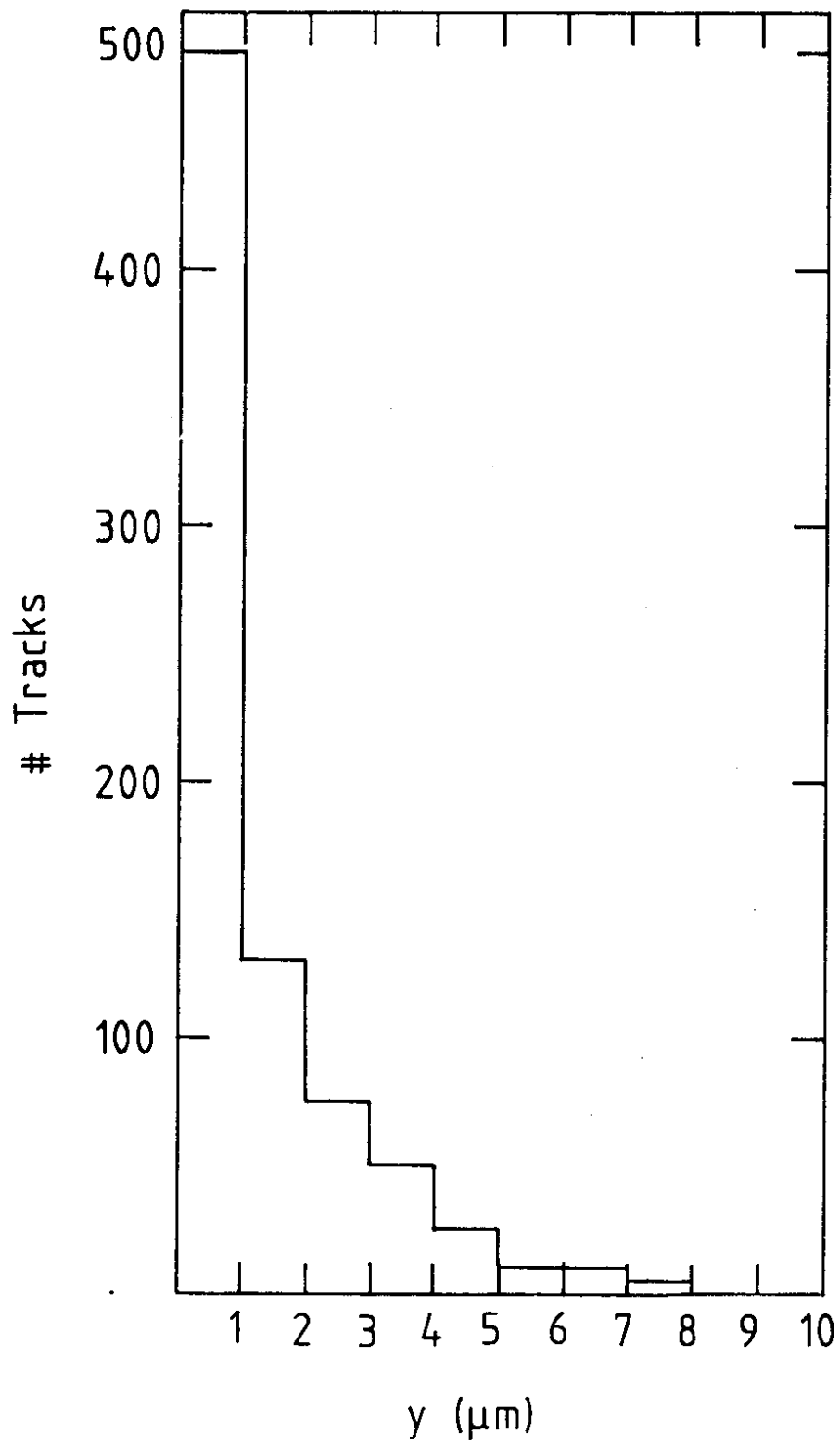


Fig. 4

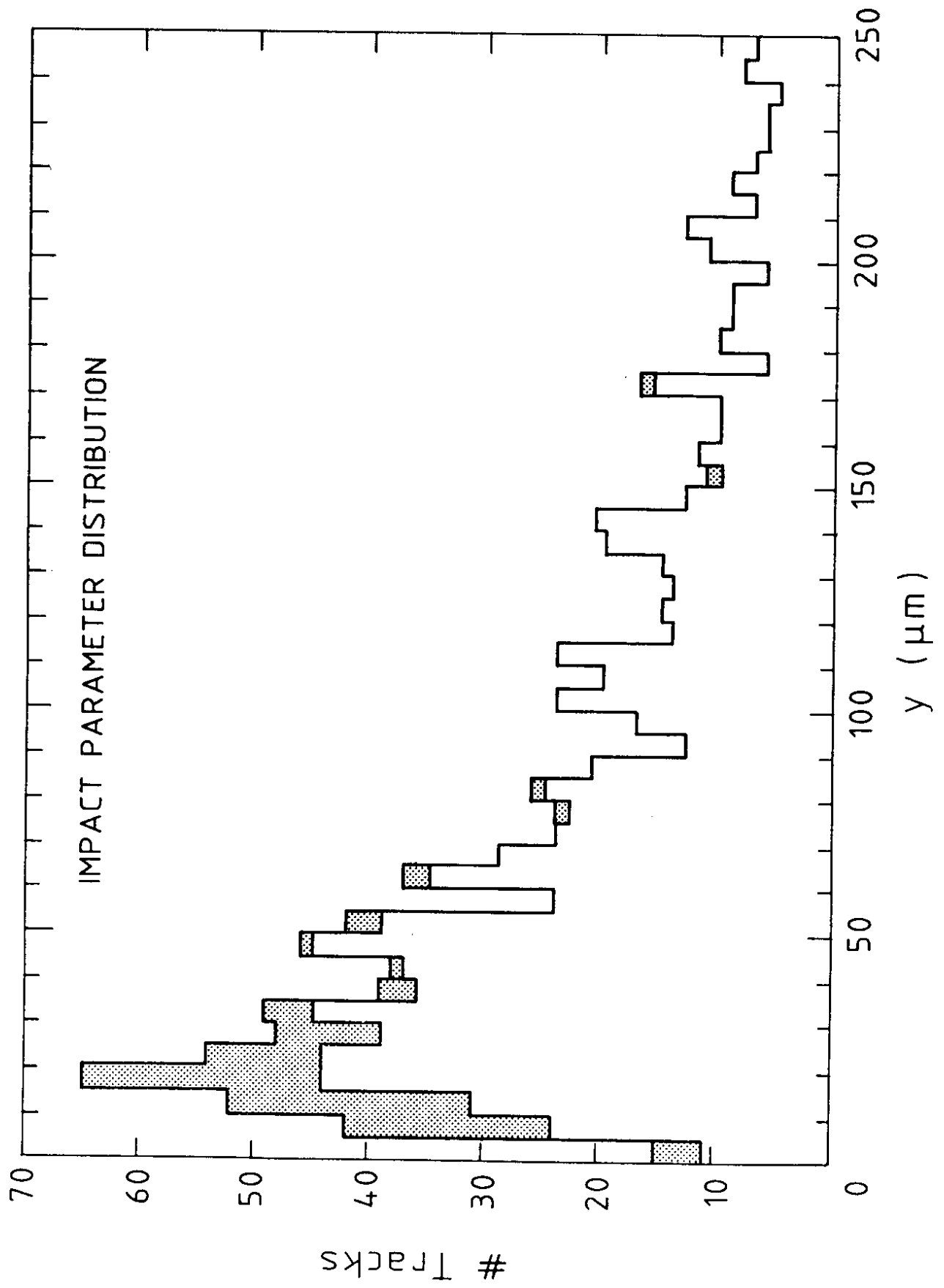


Fig. 5

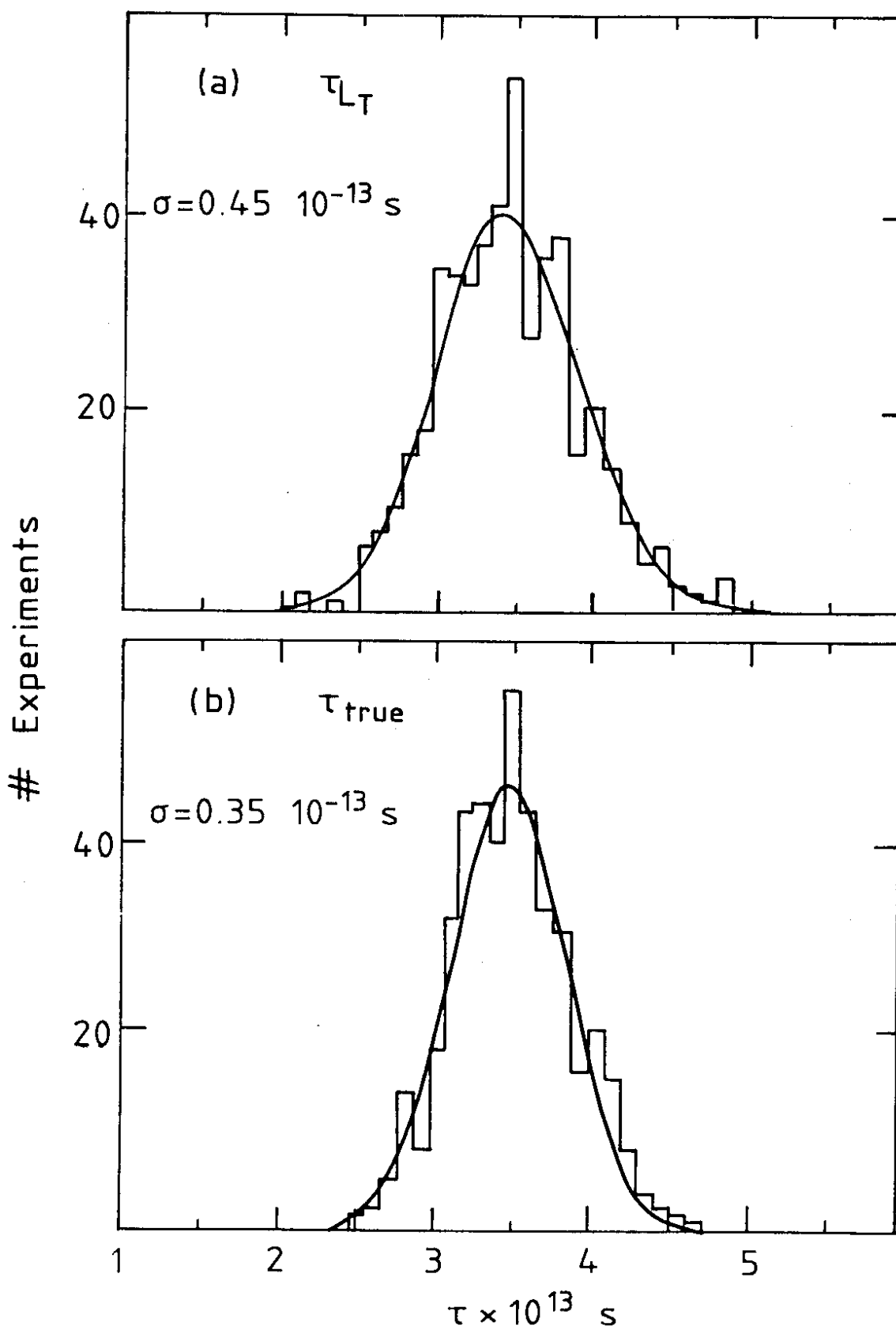


Fig. 6

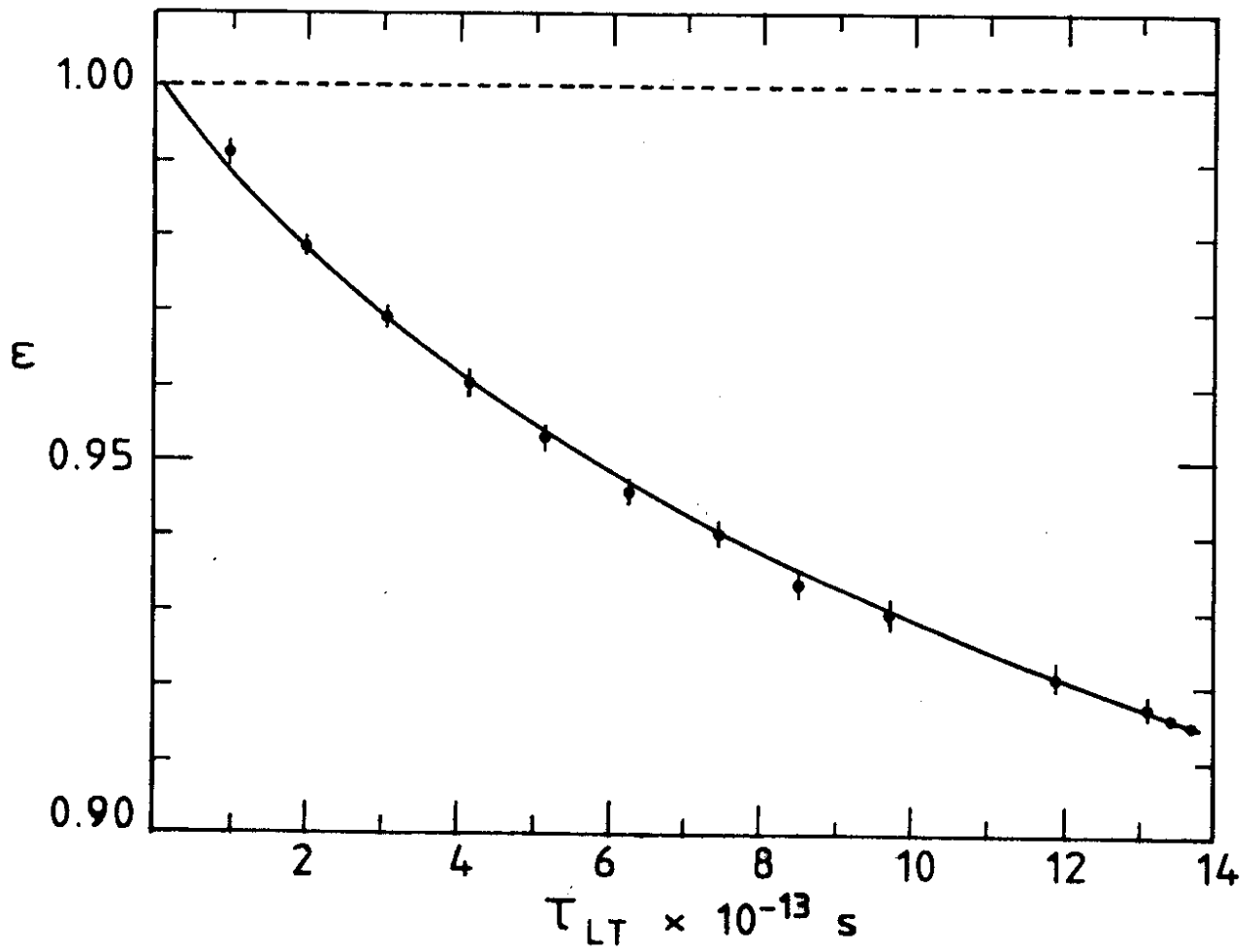


Fig. 7

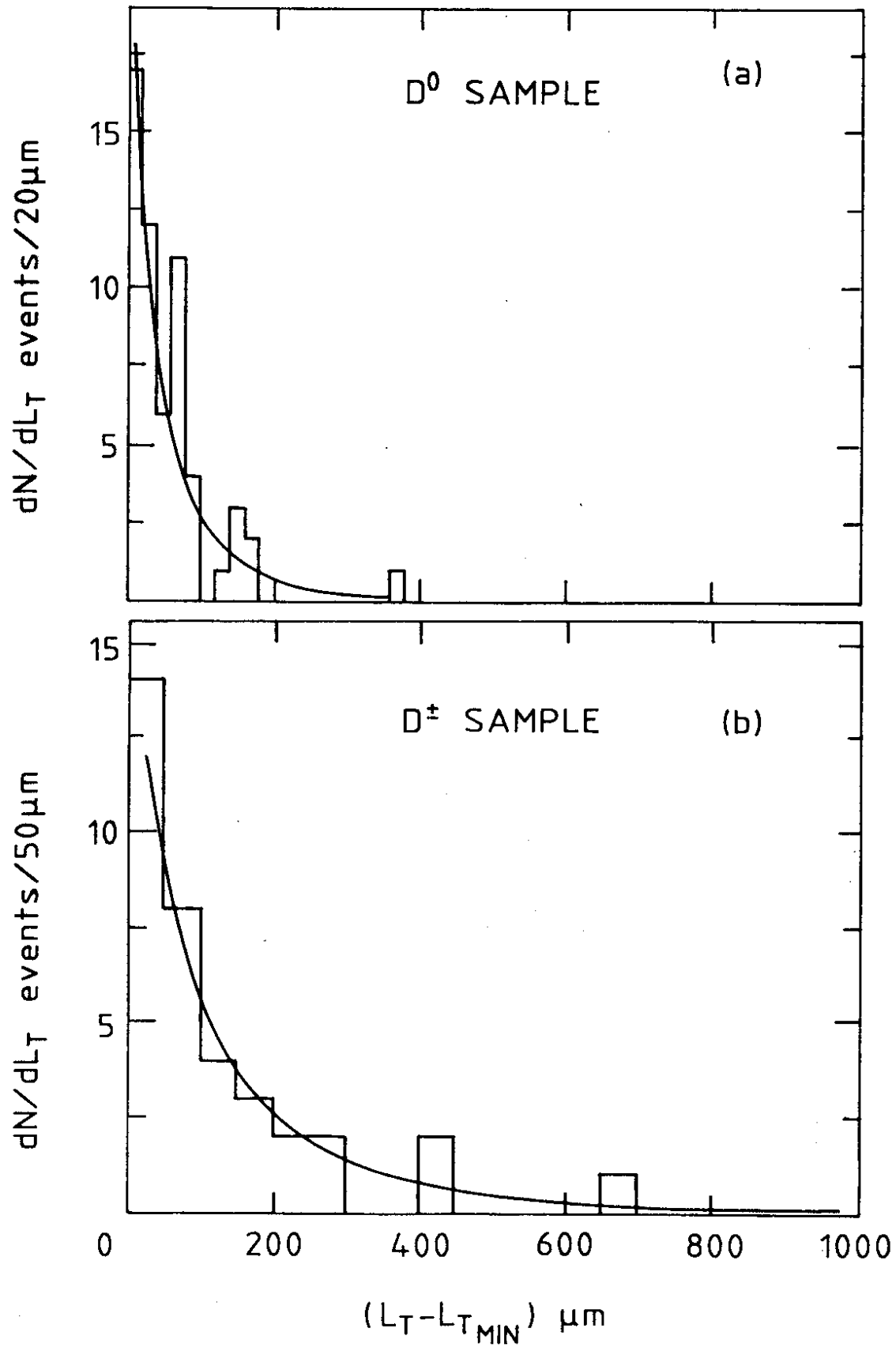


Fig. 8

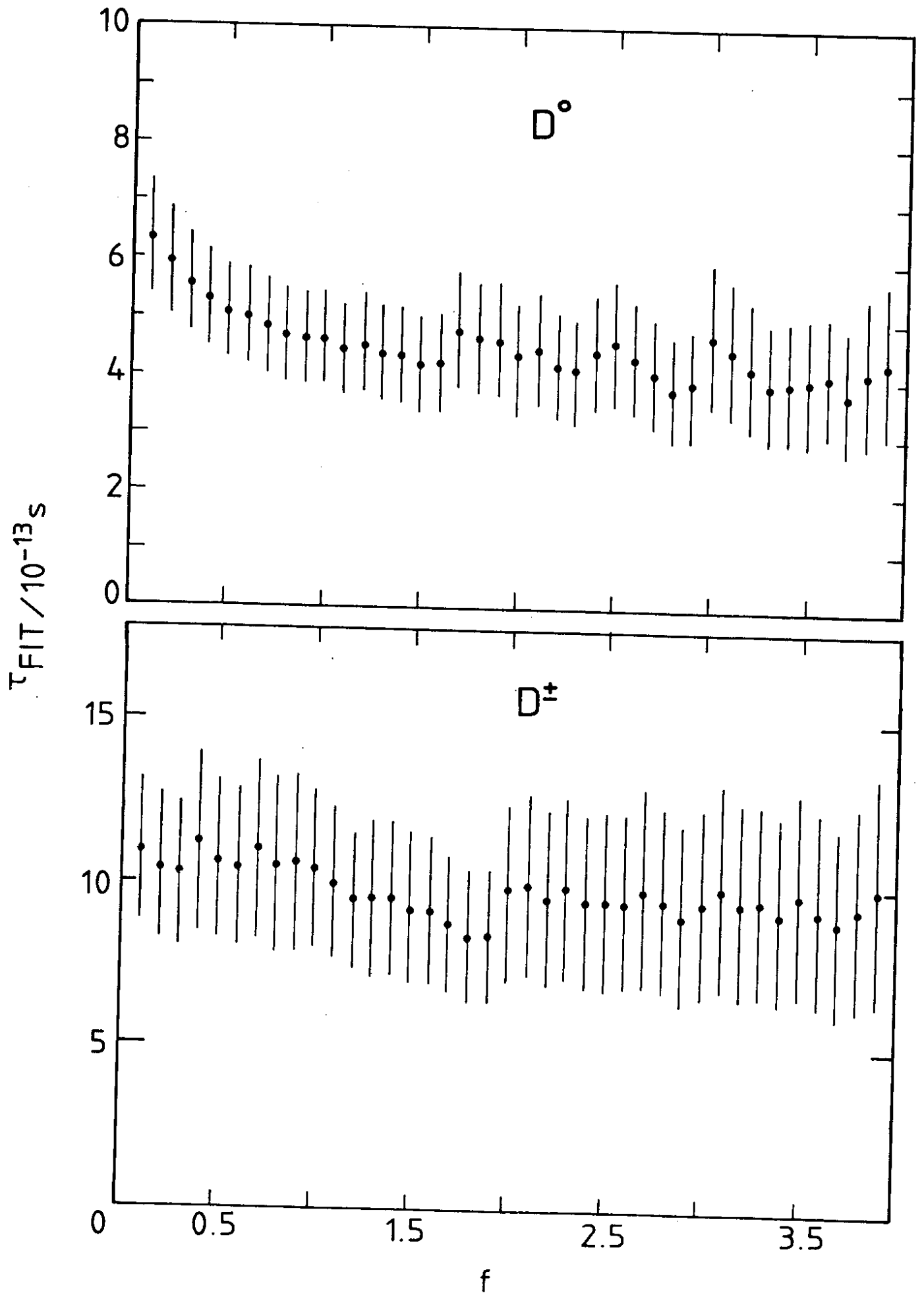


Fig. 9

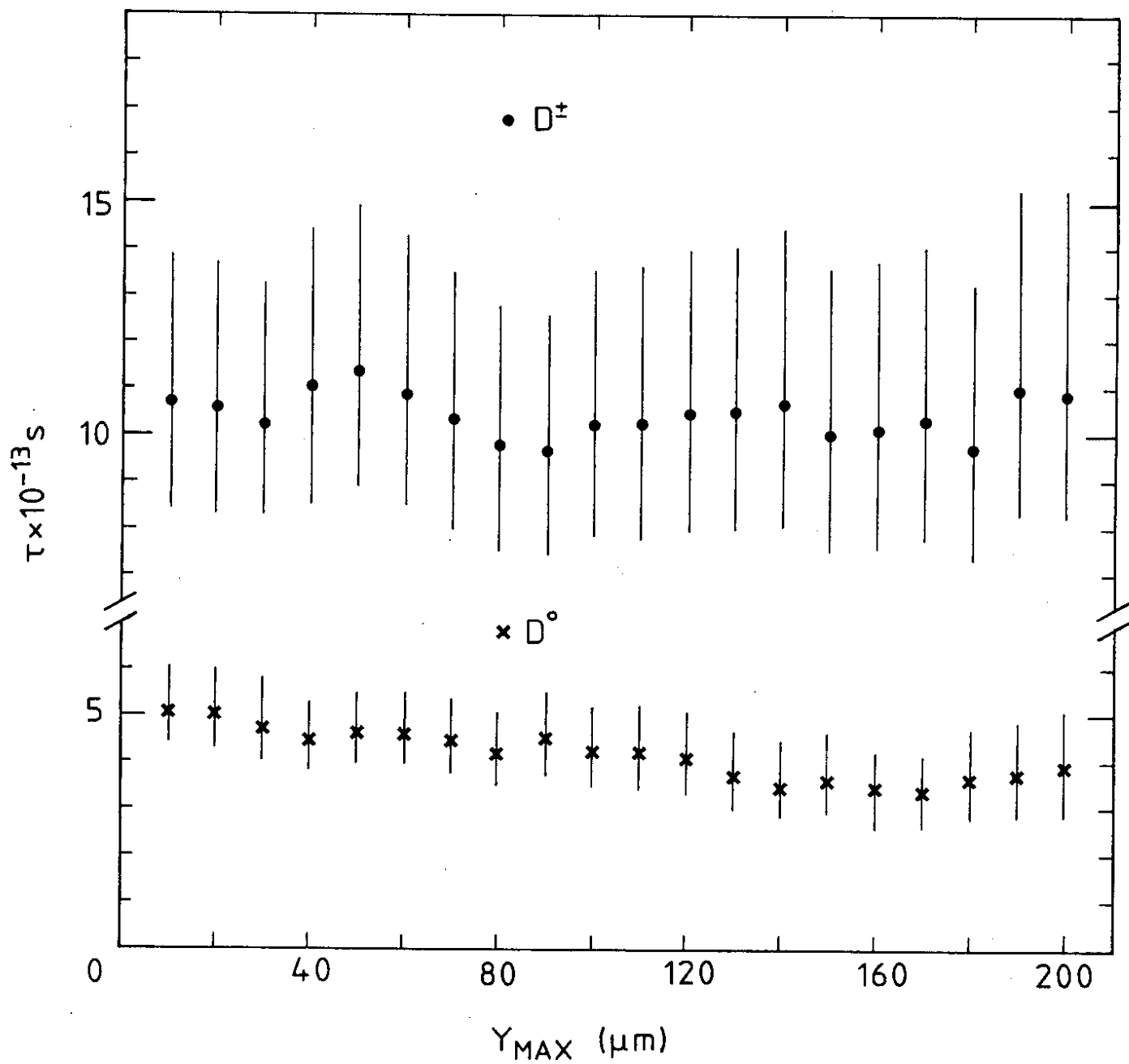


Fig. 10

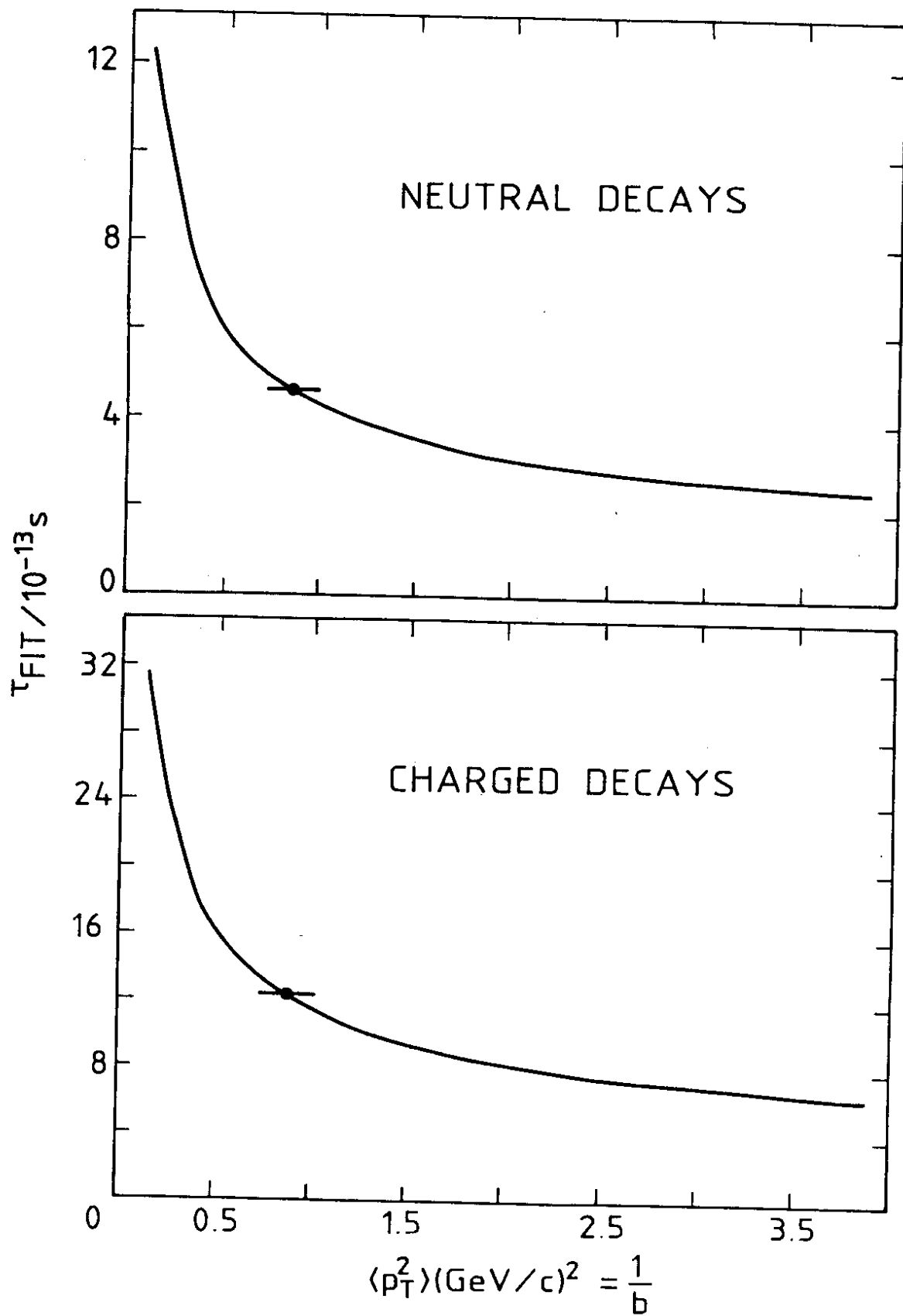


Fig. 11

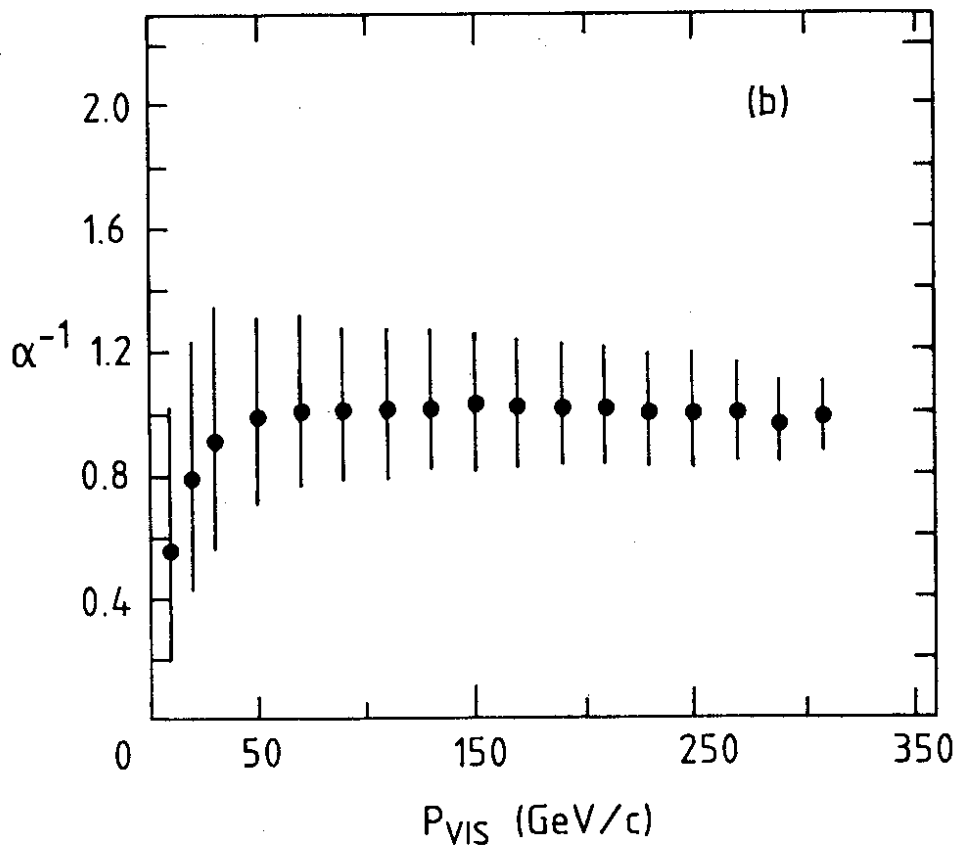
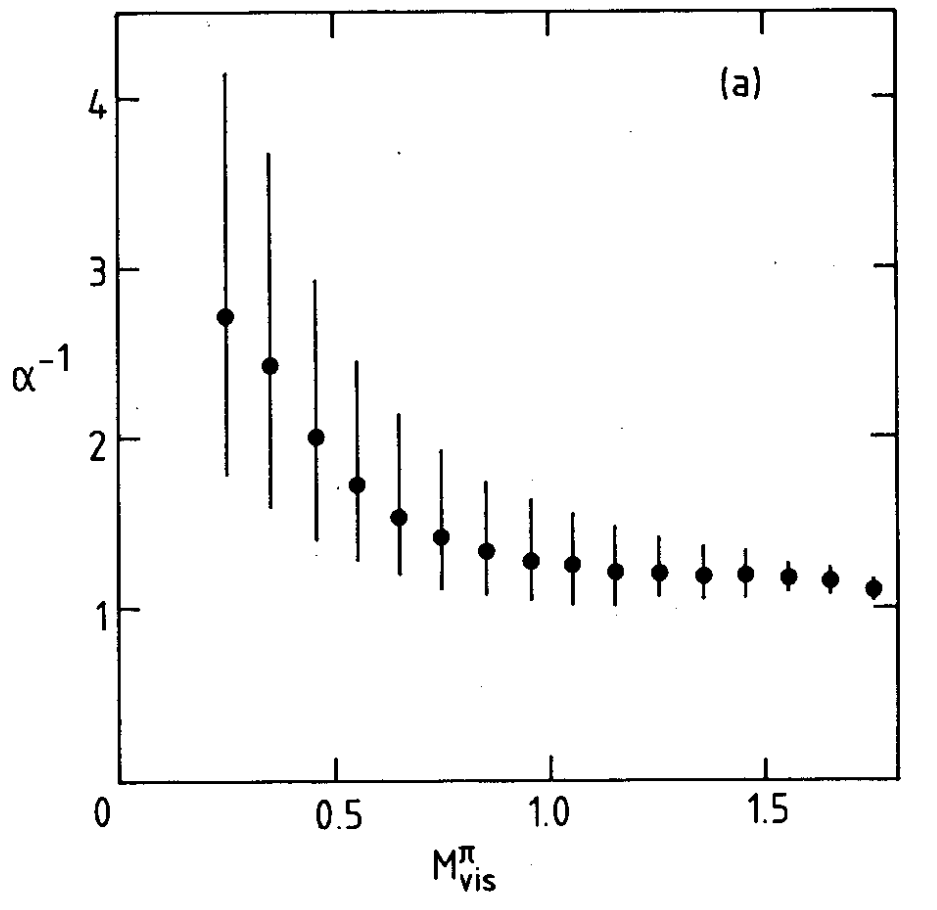


Fig. 12

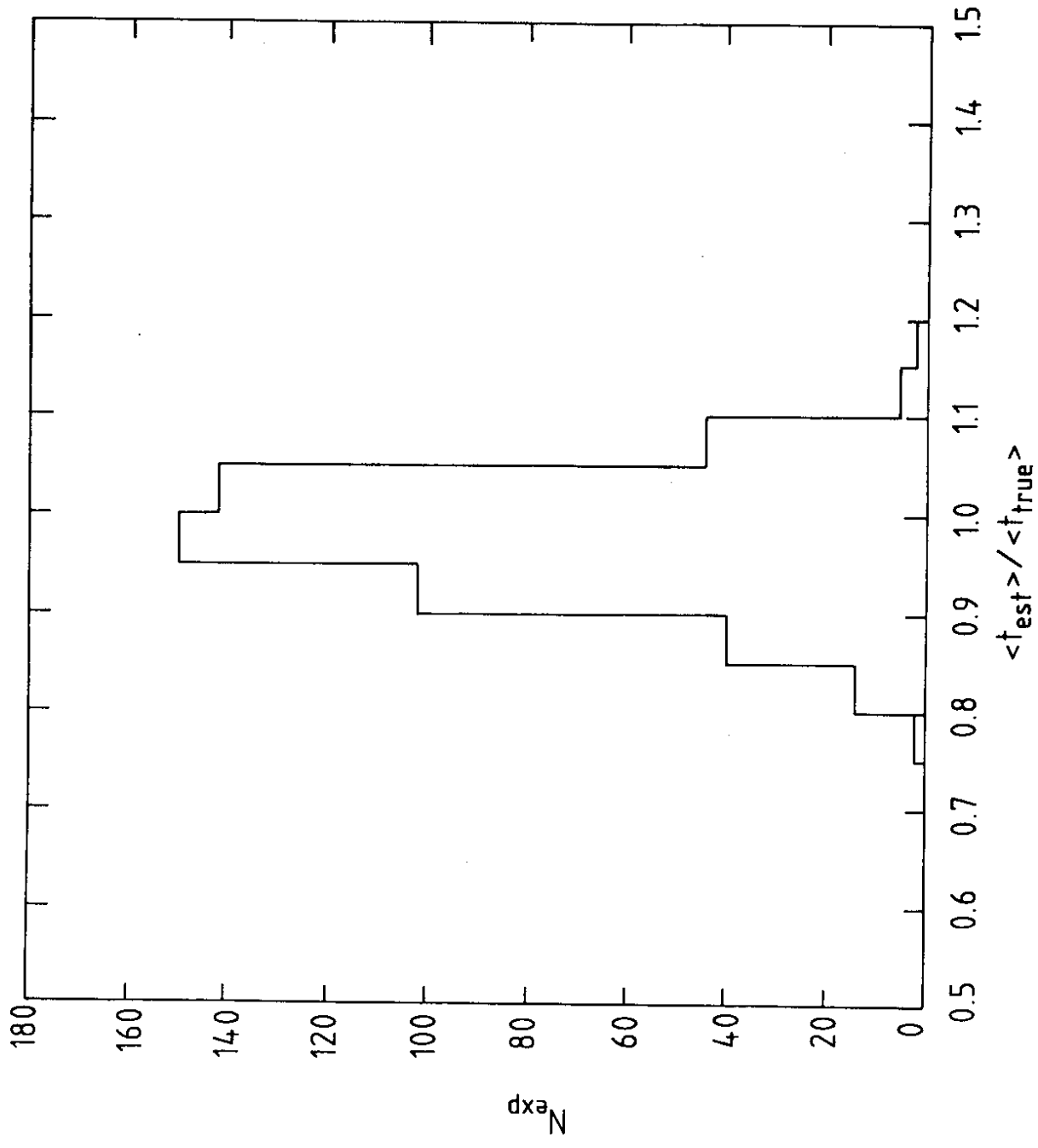


Fig. 13

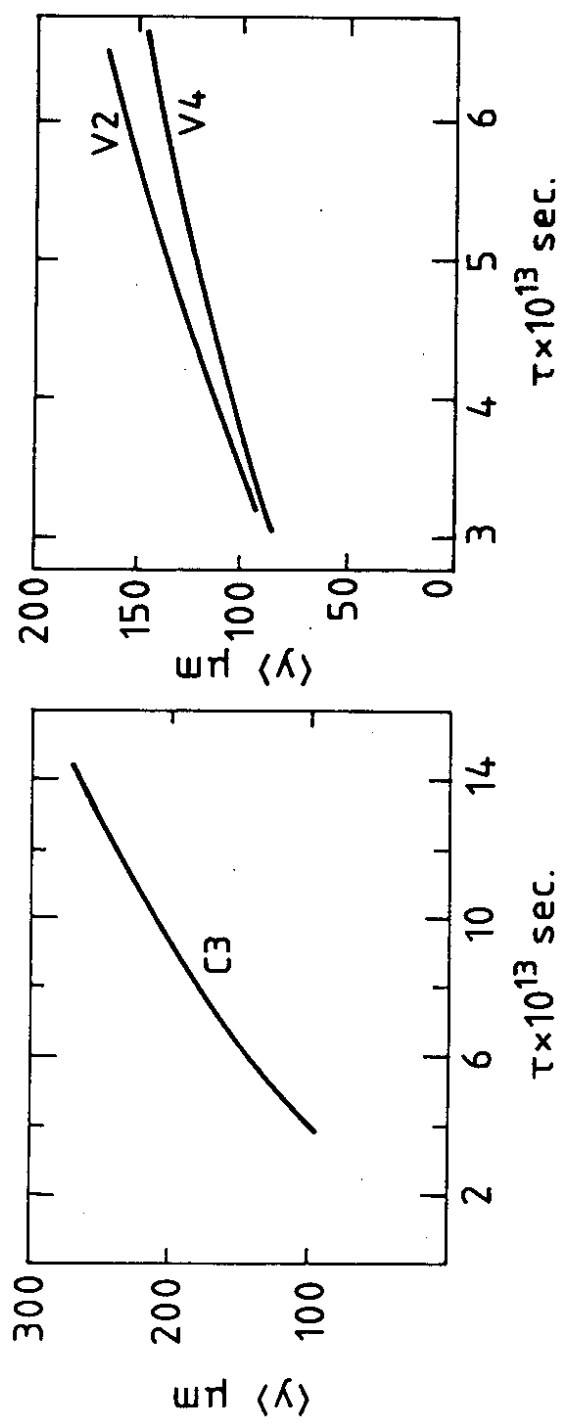


Fig. 14

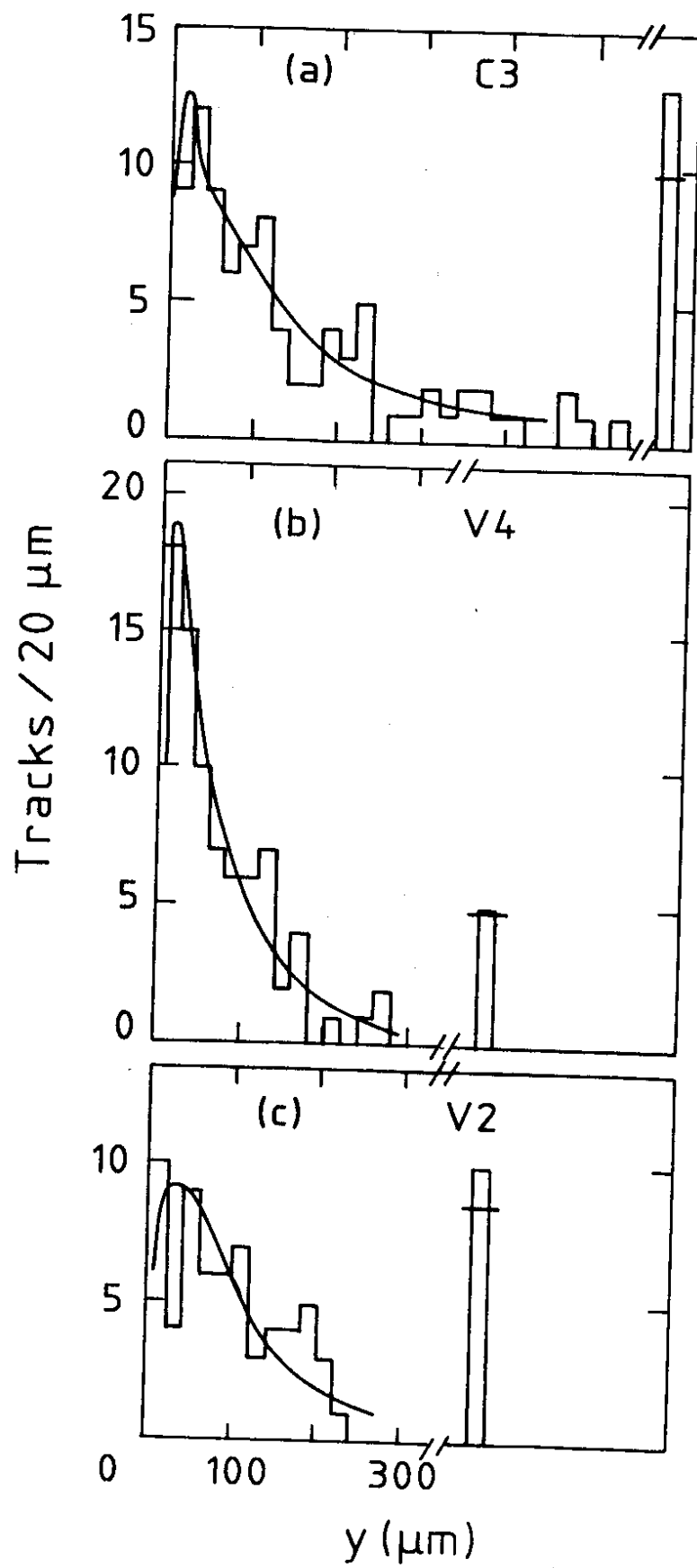


Fig. 15

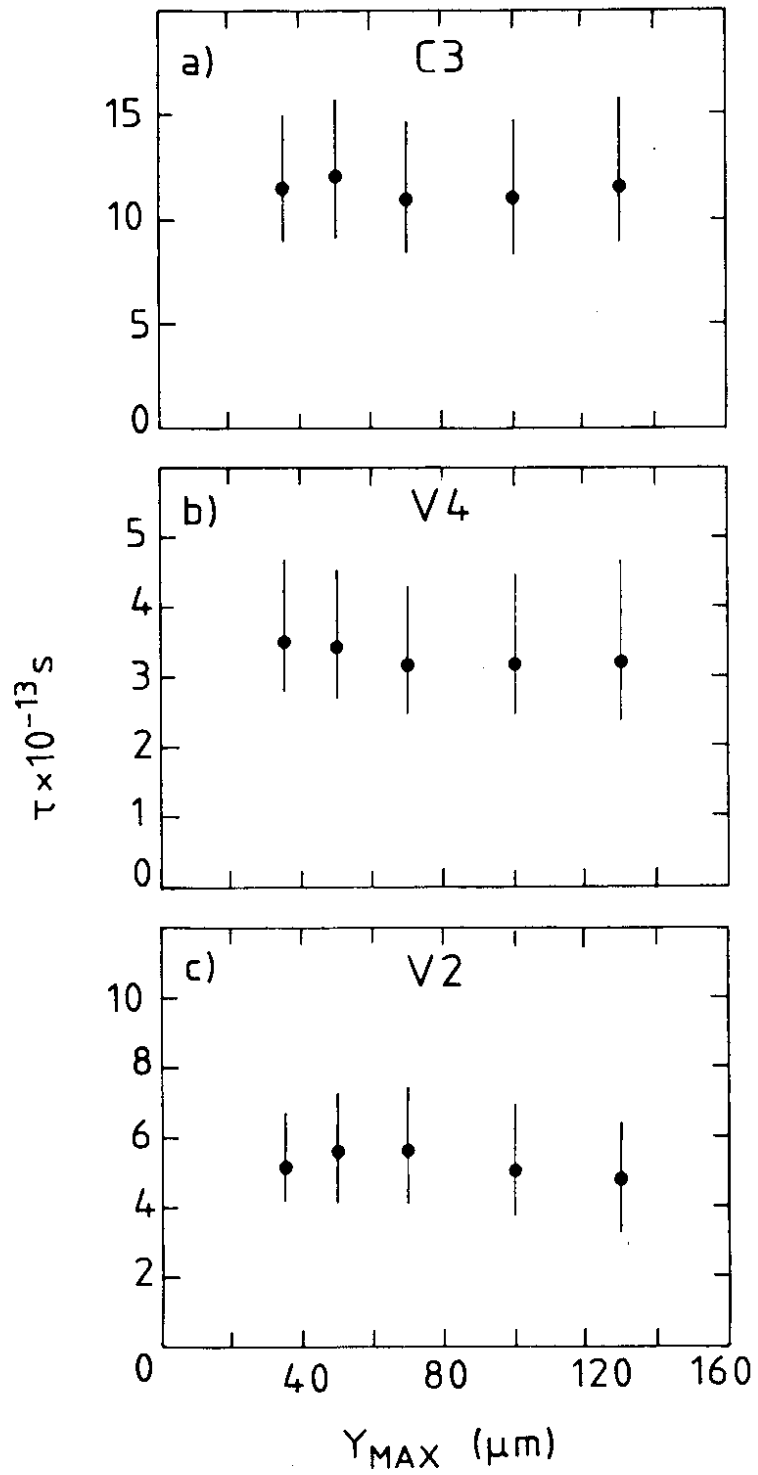


Fig. 16